helicase activities. Moreover, we clearly detected a CKB-NS4A complex using anti-tag antibodies in cotransfection experiments, but the endogenous complex could not be immunoprecipitated from cells expressing only endogenous levels of CKB, probably because of the inefficiency of the available antibodies. Further, a deletion of the NS4A-interacting region within an inactive mutant of CKB (CKB-C283S) resulted in the loss of its dominant-negative effect on HCV replication.

Creatine kinase, an evolutionarily conserved enzyme, is known to be critical for the maintenance and regulation of cellular energy stores in tissues with high and rapidly changing energy demands (48). In mammals, three cytosolic and two mitochondrial isoforms of CK, which share certain conserved regions, are expressed (35). The brain-type CK, CKB, plays a major role in cellular energy metabolism of nonmuscle cells, reversibly catalyzing the ATP-dependent phosphorylation of creatine and, hence, providing an ATP buffering system in subcellular compartments of high and fluctuating energy demand (21, 29). CKB is overexpressed in a wide range of tumor tissues and tumor cell lines, including hepatocellular carcinoma (32), and is used as a prognostic marker of cancer.

Although CK and creatine phosphate have been supplemented to in vitro replicase assays of some RNA viruses (15, 33), understanding of CKB function in the virus life cycle has been limited. One study indicated that the CK substrate analog, Ccr, exhibits antiviral activity against several herpesviruses but not influenza viruses or vesicular stomatitis virus (26). We have demonstrated here that HCV genome replication is downregulated by either treatment with Ccr, siRNA-mediated knockdown of CKB, or the exogenous expression of CKB-C283S. Coimmunoprecipitation experiments revealed that the essential domain within NS4A for the interaction with CKB is the NS4A central domain, aa 21 to 39, which is also responsible for NS3-4A complex formation. However, the NS3-4A interaction was not impaired by overexpression of CKB, and CKB was found to be able to form a complex with NS3-4A (Fig. 3H). Since CKB does not directly interact with NS3 (Fig. 3A), it is likely that NS3-4A-CKB association occurs through two interactions of NS3-4A and NS4A-CKB. We examined whether the formation of the ternary complex affects HCV enzymatic activities, possibly through conformational changes in the viral proteins, and found that CKB has no influence on NS3-4A protease activity (Fig. 5C). With regard to helicase activity, the effect of CKB on RNA unwinding activity by NS3-4A was similar to the effect of NS3 alone in the presence of ATP (Fig. 5A). It is conceivable that interaction with CKB causes no or little global change in the NS3-4A conformation and does not affect the viral helicase and protease activities.

In general, translation initiation in eukaryotes includes an ATP-dependent process such as unwinding the secondary structure in the 5′-untranslated region to permit assembly of 48S ribosomal complexes. It was reported, however, that 48S complex formation on the HCV internal ribosome entry site (IRES) has no requirement for ATP hydrolysis (25). In fact, we found that Huh-7 cells with or without gene silencing of CKB exhibited the same level of HCV IRES activity by transfection with IRES-reporter constructs (data not shown).

Collectively, we conclude that CKB is targeted to the HCV RC through its interaction with NS4A and functions as a positive regulator for the viral replicase by providing ATP. It is likely that the catalytic activity of CKB that associates with the viral RC is important for enhancing the RNA replication. The role of CKB-NS4A interaction in the enhancing effect seems to be limited. Although either knocking down CKB, expression of the dominant-negative mutant of CKB, or Ccr treatment resulted in the reduction of HCV replication (Fig. 2A to C), the total cellular ATP levels were not changed under these conditions (Fig. 2D). This suggests that CKB contributes to enhancing HCV replication through controlling the ATP level in the particular RC compartment. A tight coupling of a fast ATP regeneration and delivery system to the viral RC is advantageous for achieving efficient replication of the viral genome. To our knowledge, the findings presented here provide the first experimental evidence of the involvement of viral protein in recruiting an ATP generating/buffering system to the subcellular compartment for viral genome replication, a site with high-energy turnover. Given that the levels of HCV RNA were not dramatically diminished by the knocking down, dominant-negative mutant or Ccr, CKB may not be absolutely critical for the viral replication. One would argue that energy required for HCV genome replication can be partly complemented from the intracellular ATP pool.

Although there are several isoforms of CK as described above, the most abundant CK species expressed in Huh-7 cells in the present study was CKB, and no other isoenzymes, including mitochondrial CK, were detected by an isoform analysis based on the overlay gel technique (32; data not shown). Thus, the CKB isoenzyme appears to be a key molecule in the energy metabolism of HCV replicating cells. To identify potential HCV RC components, we used a comparative proteome analysis of the DRM fraction in cells harboring HCV subgenomic replicon and the DRM fractions in parental cells and then identified proteins that were more abundant in the fraction of HCV replicating cells. In agreement with similar previously reported approaches using the DRM or lipid raft fraction (30, 53), the functional categories of identified proteins included protein folding or assembly, cell metabolism and biosynthesis, cellular processes, and cytoskeleton organization (Table 1). Interestingly, Mannova et al. found that CKB was upregulated in the fraction of Huh-7 cells carrying the genotype 1b Con1 isolate-derived HCV replicon, as determined using stable isotope labeling by amino acids combined with one-dimensional electrophoresis (30). However, the effect of CKB on regulation of the HCV life cycle was not examined in that study.

In conclusion, CKB interacts with HCV NS4A and is important for efficient replication of the viral genome. Recruitment of CKB to the HCV replication machinery through its interaction with NS4A may have important implications for the maintenance or enhancement of the functional replicase activity in the RC compartment, where high-energy phosphoryl groups are required. A strategy for specific interception of energy supply at the subcellular site of HCV genome replication by disruption of the NS4A-CKB interface may lead to development of a new type of antiviral agent.

ACKNOWLEDGMENTS

We thank Francis V. Chisari (The Scripps Research Institute) for providing Huh-7.5.1 cells; Raffaele De Francesco (Istituto di Ricerche

di Biologia Molecolare, P. Angeletti) for providing purified recombinant NS3 and NS3-4A proteins; Oriental Yeast Co., Ltd., for providing human CKB cDNA; Minoru Fukuda (Laboratory for Electron Microscopy, Kyorin University School of Medicine) for electron microscopy; S. Yoshizaki, T. Shimoji, M. Kaga, M. Sasaki, and T. Date for technical assistance; and T. Mizoguchi for secretarial work.

This study was supported by a grant-in-aid for Scientific Research from the Japan Society for the Promotion of Science, from the Ministry of Health, Labor, and Welfare of Japan and from the Ministry of Education, Culture, Sports, Science, and Technology and by Research on Health Sciences focusing on Drug Innovation from the Japan Health Sciences Foundation, Japan, and by the Program for Promotion of Fundamental Studies in Health Sciences of the National Institute of Biomedical Innovation of Japan.

REFERENCES

1. **Aizaki, H., Y. Aoki, T. Harada, K. Ishii, T. Suzuki, S. Nagamori, G. Toda, Y. Matsuura, and T. Miyamura.** 1998. Full-length complementary DNA of hepatitis C virus genome from an infectious blood sample. Hepatology **27:** 621–627.
2. **Aizaki, H., K. J. Lee, V. M. Sung, H. Ishiko, and M. M. Lai.** 2004. Characterization of the hepatitis C virus RNA replication complex associated with lipid rafts. Virology **324:**450–461.
3. **Aizaki, H., K. Morikawa, M. Fukasawa, H. Hara, Y. Inoue, H. Tani, K. Saito, M. Nishijima, K. Hanada, Y. Matsuura, M. M. Lai, T. Miyamura, T. Wakita, and T. Suzuki.** 2008. Critical role of virion-associated cholesterol and sphingolipid in hepatitis C virus infection. J. Virol. **82:**5715–5724.
4. **Alter, H. J., and L. B. Seeff.** 2000. Recovery, persistence, and sequelae in hepatitis C virus infection: a perspective on long-term outcome. Semin. Liver Dis. **20:**17–35.
5. **Aoyagi, K., C. Ohue, K. Iida, T. Kimura, E. Tanaka, K. Kiyosawa, and S. Yagi.** 1999. Development of a simple and highly sensitive enzyme immunoassay for hepatitis C virus core antigen. J. Clin. Microbiol. **37:**1802–1808.
6. **Appel, N., T. Schaller, F. Penin, and R. Bartenschlager.** 2006. From structure to function: new insights into hepatitis C virus RNA replication. J. Biol. Chem. **281:**9833–9836.
7. **Bartenschlager, R., and V. Lohmann.** 2001. Novel cell culture systems for the hepatitis C virus. Antivir. Res. **52:**1–17.
8. **Brass, V., J. M. Berke, R. Montserret, H. E. Blum, F. Penin, and D. Moradpour.** 2008. Structural determinants for membrane association and dynamic organization of the hepatitis C virus NS3-4A complex. Proc. Natl. Acad. Sci. USA.
9. **Dumont, S., W. Cheng, V. Serebrov, R. K. Beran, I. Tinoco, Jr., A. M. Pyle, and C. Bustamante.** 2006. RNA translocation and unwinding mechanism of HCV NS3 helicase and its coordination by ATP. Nature **439:**105–108.
10. **Failla, C., L. Tomei, and R. De Francesco.** 1994. Both NS3 and NS4A are required for proteolytic processing of hepatitis C virus nonstructural proteins. J. Virol. **68:**3753–3760.
11. **Gallinari, P., D. Brennan, C. Nardi, M. Brunetti, L. Tomei, C. Steinkuhler, and R. De Francesco.** 1998. Multiple enzymatic activities associated with recombinant NS3 protein of hepatitis C virus. J. Virol. **72:**6758–6769.
12. **Gallinari, P., C. Paolini, D. Brennan, C. Nardi, C. Steinkuhler, and R. De Francesco.** 1999. Modulation of hepatitis C virus NS3 protease and helicase activities through the interaction with NS4A. Biochemistry **38:**5620–5632.
13. **Gao, L., H. Aizaki, J. W. He, and M. M. Lai.** 2004. Interactions between viral nonstructural proteins and host protein hVAP-33 mediate the formation of hepatitis C virus RNA replication complex on lipid raft. J. Virol. **78:**3480–3488.
14. **Gosert, R., D. Egger, V. Lohmann, R. Bartenschlager, H. E. Blum, K. Bienz, and D. Moradpour.** 2003. Identification of the hepatitis C virus RNA replication complex in Huh-7 cells harboring subgenomic replicons. J. Virol. **77:**5487–5492.
15. **Green, K. Y., A. Mory, M. H. Fogg, A. Weisberg, G. Belliot, M. Wagner, T. Mitra, E. Ehrenfeld, C. E. Cameron, and S. V. Sosnovtsev.** 2002. Isolation of enzymatically active replication complexes from feline calicivirus-infected cells. J. Virol. **76:**8582–8595.
16. **Guidotti, L. G., and F. V. Chisari.** 2006. Immunobiology and pathogenesis of viral hepatitis. Annu. Rev. Pathol. **1:**23–61.
17. **Guo, J. T., V. V. Bichko, and C. Seeger.** 2001. Effect of alpha interferon on the hepatitis C virus replicon. J. Virol. **75:**8516–8523.
18. **Hamamoto, I., Y. Nishimura, T. Okamoto, H. Aizaki, M. Liu, Y. Mori, T. Abe, T. Suzuki, M. M. Lai, T. Miyamura, K. Moriishi, and Y. Matsuura.** 2005. Human VAP-B is involved in hepatitis C virus replication through interaction with NS5A and NS5B. J. Virol. **79:**13473–13482.
19. **Hoofnagle, J. H.** 2002. Course and outcome of hepatitis C. Hepatology **36:**S21–S29.
20. **Ichimura, T., H. Yamamura, K. Sasamoto, Y. Tominaga, M. Taoka, K. Kakiuchi, T. Shinkawa, N. Takahashi, S. Shimada, and T. Isobe.** 2005. 14-3-3 proteins modulate the expression of epithelial Na+ channels by phosphorylation-dependent interaction with Nedd4-2 ubiquitin ligase. J. Biol. Chem. **280:**13187–13194.
21. **Inoue, K., S. Ueno, and A. Fukuda.** 2004. Interaction of neuron-specific K^+-Cl^- cotransporter, KCC2, with brain-type creatine kinase. FEBS Lett. **564:**131–135.
22. **Inoue, K., J. Yamada, S. Ueno, and A. Fukuda.** 2006. Brain-type creatine kinase activates neuron-specific K^+-Cl^- cotransporter KCC2. J. Neurochem. **96:**598–608.
23. **Kato, T., T. Date, M. Miyamoto, A. Furusaka, K. Tokushige, M. Mizokami, and T. Wakita.** 2003. Efficient replication of the genotype 2a hepatitis C virus subgenomic replicon. Gastroenterology **125:**1808–1817.
24. **Kato, T., A. Furusaka, M. Miyamoto, T. Date, K. Yasui, J. Hiramoto, K. Nagayama, T. Tanaka, and T. Wakita.** 2001. Sequence analysis of hepatitis C virus isolated from a fulminant hepatitis patient. J. Med. Virol. **64:**334–339.
25. **Lancaster, A. M., E. Jan, and P. Sarnow.** 2006. Initiation factor-independent translation mediated by the hepatitis C virus internal ribosome entry site. RNA **12:**894–902.
26. **Lillie, J. W., D. F. Smee, J. H. Huffman, L. J. Hansen, R. W. Sidwell, and R. Kaddurah-Daouk.** 1994. Cyclocreatine (1-carboxymethyl-2-iminoimidazolidine) inhibits the replication of human herpesviruses. Antivir. Res. **23:**203–218.
27. **Lindenbach, B. D., M. J. Evans, A. J. Syder, B. Wolk, T. L. Tellinghuisen, C. C. Liu, T. Maruyama, R. O. Hynes, D. R. Burton, J. A. McKeating, and C. M. Rice.** 2005. Complete replication of hepatitis C virus in cell culture. Science **309:**623–626.
28. **Lindenbach, B. D., B. M. Pragai, R. Montserret, R. K. Beran, A. M. Pyle, F. Penin, and C. M. Rice.** 2007. The C terminus of hepatitis C virus NS4A encodes an electrostatic switch that regulates NS5A hyperphosphorylation and viral replication. J. Virol. **81:**8905–8918.
29. **Mahajan, V. B., K. S. Pai, A. Lau, and D. D. Cunningham.** 2000. Creatine kinase, an ATP-generating enzyme, is required for thrombin receptor signaling to the cytoskeleton. Proc. Natl. Acad. Sci. USA **97:**12062–12067.
30. **Mannova, P., R. Fang, H. Wang, B. Deng, M. W. McIntosh, S. M. Hanash, and L. Beretta.** 2006. Modification of host lipid raft proteome upon hepatitis C virus replication. Mol. Cell Proteomics **5:**2319–2325.
31. **Manos, P., and J. Edmond.** 1992. Immunofluorescent analysis of creatine kinase in cultured astrocytes by conventional and confocal microscopy: a nuclear localization. J. Comp. Neurol. **326:**273–282.
32. **Meffert, G., F. N. Gellerich, R. Margreiter, and M. Wyss.** 2005. Elevated creatine kinase activity in primary hepatocellular carcinoma. BMC Gastroenterol. **5:**9.
33. **Miyanari, Y., M. Hijikata, M. Yamaji, M. Hosaka, H. Takahashi, and K. Shimotohno.** 2003. Hepatitis C virus nonstructural proteins in the probable membranous compartment function in viral genome replication. J. Biol. Chem. **278:**50301–50308.
34. **Moradpour, D., F. Penin, and C. M. Rice.** 2007. Replication of hepatitis C virus. Nat. Rev. Microbiol. **5:**453–463.
35. **Muhlebach, S. M., M. Gross, T. Wirz, T. Wallimann, J. C. Perriard, and M. Wyss.** 1994. Sequence homology and structure predictions of the creatine kinase isoenzymes. Mol. Cell Biochem. **133–134:**245–262.
36. **Murakami, K., K. Ishii, Y. Ishihara, S. Yoshizaki, K. Tanaka, Y. Gotoh, H. Aizaki, M. Kohara, H. Yoshioka, Y. Mori, N. Manabe, I. Shoji, T. Sata, R. Bartenschlager, Y. Matsuura, T. Miyamura, and T. Suzuki.** 2006. Production of infectious hepatitis C virus particles in three-dimensional cultures of the cell line carrying the genome-length dicistronic viral RNA of genotype 1b. Virology **351:**381–392.
37. **Nomura-Takigawa, Y., M. Nagano-Fujii, L. Deng, S. Kitazawa, S. Ishido, K. Sada, and H. Hotta.** 2006. Non-structural protein 4A of Hepatitis C virus accumulates on mitochondria and renders the cells prone to undergoing mitochondria-mediated apoptosis. J. Gen. Virol. **87:**1935–1945.
38. **Ohara-Imaizumi, M., T. Fujiwara, Y. Nakamichi, T. Okamura, Y. Akimoto, J. Kawai, S. Matsushima, H. Kawakami, T. Watanabe, K. Akagawa, and S. Nagamatsu.** 2007. Imaging analysis reveals mechanistic differences between first- and second-phase insulin exocytosis. J. Cell Biol. **177:**695–705.
39. **Okamoto, T., Y. Nishimura, T. Ichimura, K. Suzuki, T. Miyamura, T. Suzuki, K. Moriishi, and Y. Matsuura.** 2006. Hepatitis C virus RNA replication is regulated by FKBP8 and Hsp90. EMBO J. **25:**5015–5025.
40. **Oliver, I. T.** 1955. A spectrophotometric method for the determination of creatine phosphokinase and myokinase. Biochem. J. **61:**116–122.
41. **Shi, S. T., K. J. Lee, H. Aizaki, S. B. Hwang, and M. M. Lai.** 2003. Hepatitis C virus RNA replication occurs on a detergent-resistant membrane that cofractionates with caveolin-2. J. Virol. **77:**4160–4168.
42. **Shirakura, M., K. Murakami, T. Ichimura, R. Suzuki, T. Shimoji, K. Fukuda, K. Abe, S. Sato, M. Fukasawa, Y. Yamakawa, M. Nishijima, K. Moriishi, Y. Matsuura, T. Wakita, T. Suzuki, P. M. Howley, T. Miyamura, and I. Shoji.** 2007. E6AP ubiquitin ligase mediates ubiquitylation and degradation of hepatitis C virus core protein. J. Virol. **81:**1174–1185.
43. **Sunahara, Y., K. Uchida, T. Tanaka, H. Matsukawa, M. Inagaki, and Y. Matuo.** 2001. Production of recombinant human creatine kinase (r-hCK) isozymes by tandem repeat expression of M and B genes and characterization of r-hCK-MB. Clin. Chem. **47:**471–476.

44. **Suzuki, T., K. Ishii, H. Aizaki, and T. Wakita.** 2007. Hepatitis C viral life cycle. Adv. Drug Deliv. Rev. **59**:1200–1212.
45. **Taguwa, S., T. Okamoto, T. Abe, Y. Mori, T. Suzuki, K. Moriishi, and Y. Matsuura.** 2008. Human butyrate-induced transcript 1 interacts with hepatitis C virus NS5A and regulates viral replication. J. Virol. **82**:2631–2641.
46. **Takeuchi, T., A. Katsume, T. Tanaka, A. Abe, K. Inoue, K. Tsukiyama-Kohara, R. Kawaguchi, S. Tanaka, and M. Kohara.** 1999. Real-time detection system for quantification of hepatitis C virus genome. Gastroenterology **116**:636–642.
47. **Wakita, T., T. Pietschmann, T. Kato, T. Date, M. Miyamoto, Z. Zhao, K. Murthy, A. Habermann, H. G. Krausslich, M. Mizokami, R. Bartenschlager, and T. J. Liang.** 2005. Production of infectious hepatitis C virus in tissue culture from a cloned viral genome. Nat. Med. **11**:791–796.
48. **Wallimann, T., M. Wyss, D. Brdiczka, K. Nicolay, and H. M. Eppenberger.** 1992. Intracellular compartmentation, structure and function of creatine kinase isoenzymes in tissues with high and fluctuating energy demands: the 'phosphocreatine circuit' for cellular energy homeostasis. Biochem. J. **281**(Pt. 1):21–40.
49. **Watashi, K., N. Ishii, M. Hijikata, D. Inoue, T. Murata, Y. Miyanari, and K. Shimotohno.** 2005. Cyclophilin B is a functional regulator of hepatitis C virus RNA polymerase. Mol. Cell **19**:111–122.
50. **Wolk, B., D. Sansonno, H. G. Krausslich, F. Dammacco, C. M. Rice, H. E. Blum, and D. Moradpour.** 2000. Subcellular localization, stability, and trans-cleavage competence of the hepatitis C virus NS3-NS4A complex expressed in tetracycline-regulated cell lines. J. Virol. **74**:2293–2304.
51. **Wyss, M., and R. Kaddurah-Daouk.** 2000. Creatine and creatinine metabolism. Physiol. Rev. **80**:1107–1213.
52. **Yi, M., R. A. Villanueva, D. L. Thomas, T. Wakita, and S. M. Lemon.** 2006. Production of infectious genotype 1a hepatitis C virus (Hutchinson strain) in cultured human hepatoma cells. Proc. Natl. Acad. Sci. USA **103**:2310–2315.
53. **Yi, Z., C. Fang, T. Pan, J. Wang, P. Yang, and Z. Yuan.** 2006. Subproteomic study of hepatitis C virus replicon reveals Ras-GTPase-activating protein binding protein 1 as potential HCV RC component. Biochem. Biophys. Res. Commun. **350**:174–178.
54. **Zhong, J., P. Gastaminza, G. Cheng, S. Kapadia, T. Kato, D. R. Burton, S. F. Wieland, S. L. Uprichard, T. Wakita, and F. V. Chisari.** 2005. Robust hepatitis C virus infection in vitro. Proc. Natl. Acad. Sci. USA **102**:9294–9299.

JOURNAL OF VIROLOGY, Aug. 2009, p. 7959–7969 Vol. 83, No. 16
0022-538X/09/$08.00+0 doi:10.1128/JVI.00889-09

Human VAP-C Negatively Regulates Hepatitis C Virus Propagation[▽]

Hiroshi Kukihara,[1] Kohji Moriishi,[1] Shuhei Taguwa,[1] Hideki Tani,[1] Takayuki Abe,[1] Yoshio Mori,[1] Tetsuro Suzuki,[2] Takasuke Fukuhara,[1,3] Akinobu Taketomi,[3] Yoshihiko Maehara,[3] and Yoshiharu Matsuura[1]*

Department of Molecular Virology, Research Institute for Microbial Diseases, Osaka University, Osaka,[1] Department of Virology II, National Institute of Infectious Diseases, Tokyo,[2] and Department of Surgery and Science, Graduate School of Medical Sciences, Kyushu University, Fukuoka,[3] Japan

Received 3 May 2009/Accepted 2 June 2009

Human vesicle-associated membrane protein-associated protein (VAP) subtype A (VAP-A) and subtype B (VAP-B) are involved in the regulation of membrane trafficking, lipid transport and metabolism, and the unfolded protein response. VAP-A and VAP-B consist of the major sperm protein (MSP) domain, the coiled-coil motif, and the C-terminal transmembrane anchor and form homo- and heterodimers through the transmembrane domain. VAP-A and VAP-B interact with NS5B and NS5A of hepatitis C virus (HCV) through the MSP domain and the coiled-coil motif, respectively, and participate in the replication of HCV. VAP-C is a splicing variant of VAP-B consisting of the N-terminal half of the MSP domain of VAP-B followed by the subtype-specific frameshift sequences, and its biological function has not been well characterized. In this study, we have examined the biological functions of VAP-C in the propagation of HCV. VAP-C interacted with NS5B but not with VAP-A, VAP-B, or NS5A in immunoprecipitation analyses, and the expression of VAP-C inhibited the interaction of NS5B with VAP-A or VAP-B. Overexpression of VAP-C impaired the RNA replication of the HCV replicon and the propagation of the HCV JFH1 strain, whereas overexpression of VAP-A and VAP-B enhanced the replication. Furthermore, the expression of VAP-C was observed in various tissues, whereas it was barely detected in the liver. These results suggest that VAP-C acts as a negative regulator of HCV propagation and that the expression of VAP-C may participate in the determination of tissue tropism of HCV propagation.

Hepatitis C virus (HCV) is a major causative agent of chronic liver disease and thus a major public health problem, infecting at least 3% of the world population (47). HCV infection proceeds to the persistent stage in approximately 80% of patients, leading to the development of cirrhosis in 20% to 50% of patients, of whom approximately 5% eventually develop hepatocellular carcinoma (12). HCV encompasses a single-stranded positive-sense RNA genome of approximately 9.6 kb, which encodes a large precursor polyprotein comprising approximately 3,000 amino acids (26). The structural proteins are cleaved from the N-terminal one-fourth of the polyprotein by the host signal peptidase and signal peptide peptidase (23, 32, 33), resulting in the maturation of the capsid protein, two envelope proteins and viroporin p7. The NS2 protease cleaves after the carboxyl terminus, and then NS3 cleaves the appropriate downstream positions to produce NS4A, NS4B, NS5A, and NS5B (8, 42), all of which form the replication complex along with several host proteins (5, 21). NS5B is the RNA-dependent RNA polymerase, which is a main enzymatic component of the replication complex of HCV (3), while NS5A is a membrane-anchored zinc-binding phosphoprotein that appears to possess diverse functions, including the suppression of host defense and the regulation of the virus's replication (1, 4, 6, 41), although its biological function remains unclear.

* Corresponding author. Mailing address: Department of Molecular Virology, Research Institute for Microbial Diseases, Osaka University, 3-1, Yamadaoka, Suita, Osaka 565-0871, Japan. Phone: 81-6-6879-8340. Fax: 81-6-6879-8269. E-mail: matsuura@biken.osaka-u.ac.jp.

▽ Published ahead of print on 10 June 2009.

The NS5A protein has been shown to interact with several host proteins, including vesicle-associated membrane protein (VAMP)-associated protein (VAP) subtype A (VAP-A) (44) and subtype B (VAP-B) (9), FKBP8 (34), MyD88 (1), FBL2 (46), human butyrate-induced transcript 1 (hB-ind1) (40), and so on (25). VAP-A and VAP-B also bind to NS5B, although it remains unclear whether these interactions modulate HCV replication positively or negatively (9, 44). VAP-A and VAP-B have been shown to associate with the cytoplasmic face of the endoplasmic reticulum (ER) and the Golgi apparatus (38) and to consist of the major sperm protein (MSP) domain, the coiled-coil domain, and the transmembrane (TM) region, in that order (30, 39), as shown in Fig. 1A. VAP was originally reported as a protein binding to VAMP, which is a synaptic vesicle SNARE protein required for synaptic-vesicle fusion in the nematode *Aplysia californica*, and was designated the 33-kDa VAMP-associated protein, VAP-33 (39). Two mammalian homologues, VAP-A and VAP-B, were subsequently identified (30, 38). The transcription of VAP-A and VAP-B is ubiquitously detected in mammalian organs, including the heart, placenta, lung, liver, skeletal muscle, and pancreas (30), suggesting that VAP family proteins are involved in diverse cellular functions other than neurotransmitter release (30, 38, 49). Several VAP-interacting proteins share the FFAT motif (two phenylalanines in an acidic tract), which has the consensus amino acid sequence EFFDAXE, as determined by a comparison among oxysterol binding proteins (OSBPs), OSBP-related proteins (ORPs) (20), and the ceramide transport protein CERT (10, 19), contributing to the regulation of fatty acid metabolism. The interaction of VAP family proteins with

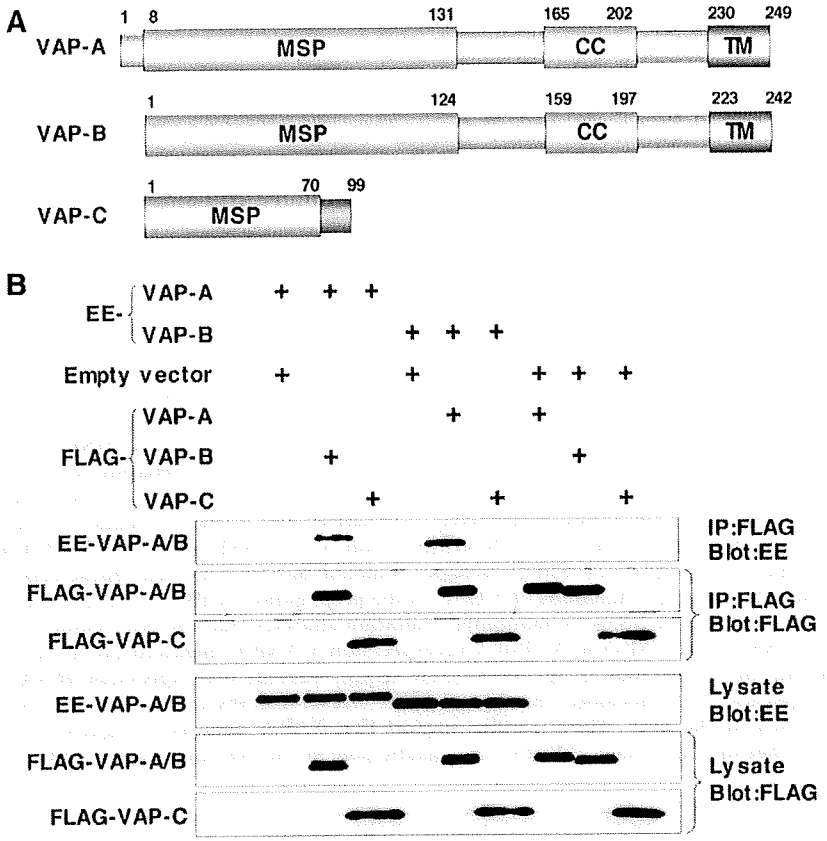

FIG. 1. VAP-C interacts with neither VAP-A nor VAP-B. (A) Structures of VAP family proteins. The MSP domain, the coiled-coil domain, and the TM region are indicated as MSP, CC, and TM, respectively. (B) Interaction among VAP family proteins. The expression plasmids encoding VAP proteins or empty vector (1 μg each) were transfected into 293T cells, FLAG-tagged VAP proteins coexpressed with EE-tagged VAP-A or VAP-B were immunoprecipitated (IP) with anti-FLAG antibody, and the resulting precipitates were examined by immunoblotting using anti-FLAG or anti-EE antibody. One percent of the volume of the lysate was used as an input control. The data in each panel are representative of the results of three independent experiments. +, present.

other host proteins, including VAMP and tubulin, is independent of the FFAT motif (16, 36, 38, 50). The third subtype of VAP is VAP-C, which is an alternative spliced isoform of VAP-B, consisting of the N-terminal half of the MSP domain and the subtype-specific 29 amino acids (Fig. 1A). However, its tissue distribution and physiological function remain largely unknown.

Glutathione *S*-transferase pulldown and immunoprecipitation analyses revealed that both VAP-A and VAP-B interact with NS5B and NS5A through the MSP domain and the coiled-coil domain, respectively (9, 44), and the MSP domains of VAP-A and VAP-B exhibit 82.3% homology. Although VAP-C possesses the N-terminal-half region of the MSP domain of VAP-B, the biological significance of VAP-C in the propagation of HCV has not yet been clarified. In this study, we examined the expression of VAP-C in human tissues and the effects of VAP-C expression on the RNA replication, translation, and particle formation of HCV.

MATERIALS AND METHODS

Cell lines. Cells of the human hepatoma cell line Huh-7, cell line Huh7OK1, and embryonic kidney cell line 293T were maintained in Dulbecco's modified Eagle's medium (DMEM) (Sigma, St. Louis, MO) containing 10% fetal calf serum (FCS) and nonessential amino acids (NEAA), while Huh 9-13 cells, which possess a subgenomic HCV RNA replicon of genotype 1b (21), were cultured in DMEM supplemented with 10% FCS, NEAA, and 1 mg/ml G418. The Huh7OK1 cell line exhibits the highest efficiency of propagation of strain JFH1 virus, as described previously (35). All cell lines were cultured at 37°C in a humidified atmosphere with 5% CO_2.

Antibodies. Chicken anti-human VAP-B antibody was described previously (9). Rabbit anti-human VAP-C antibody was prepared by immunization using synthetic peptides of the amino acid residues from 86 to 98, QPHFSISPNW EGR, which region does not share the homology to VAP-A and VAP-B. The mouse monoclonal antibody to human VAP-A was purchased from BD Pharmingen (San Diego, CA). Mouse monoclonal antibodies to influenza virus hemagglutinin (HA) and the GluGlu (EE) tag were from Covance (Richmond, CA). Mouse and rabbit anti-FLAG antibodies and mouse anti-β-actin monoclonal antibody were from Sigma. Rabbit polyclonal antibody to NS5A was prepared as described previously (34). Mouse anti-NS5A monoclonal antibody was from Austral Biologicals (San Ramon, CA).

Plasmids. A cDNA clone encoding NS5A was amplified from HCV genotype 1b strain J1 (9) (GenBank database accession number D89815) by PCR, using *Pfu* turbo DNA polymerase (Stratagene, La Jolla, CA). The fragments were then cloned into the appropriate sites in pEF-FLAG pGBK puro (13). The DNA fragment encoding NS5B of the J1 strain was generated by PCR and cloned into pCAGGs-PUR (31). The DNA fragment encoding human VAP-A was amplified by PCR from a human fetal-brain library (Clontech, Palo Alto, CA) and was introduced into pEF-FLAG pGBK puro and pEF-EE hygro (13), as described previously (9). A DNA fragment encoding VAP-C was amplified from cDNA of hepatoma cell line Huh-7 and was introduced into pEF-FLAG pGBK puro. Pro^{56}-to-Ser (P56S) mutants of VAPs were generated by site-directed mutagen-

esis (11). All PCR products were confirmed by sequencing with an ABI Prism 3130 genetic analyzer (Applied Biosystems, Tokyo, Japan).

Transfection, immunoblotting, and immunoprecipitation. Cells were seeded onto a six-well tissue culture plate 24 h before transfection. The plasmids were transfected into cells by liposome-mediated transfection using TransIT LT1 (Mirus Bio, Madison, WI). These transfected cells were harvested at 36 h post-transfection, washed three times with 1 ml of ice-cold phosphate-buffered saline (PBS), and suspended in 0.2 ml lysis buffer (20 mM Tris-HCl, pH 7.4, containing 135 mM NaCl and 1% Triton X-100) supplemented with protease inhibitor cocktail (Roche, Indianapolis, IN). The cell lysates were sonicated at 4°C for 5 min, incubated for 30 min at 4°C, and centrifuged at 15,000 rpm for 30 min at 4°C. The supernatant was subjected to immunoprecipitation analyses as described previously (27). The immunoprecipitated proteins were boiled in 30 μl of loading buffer and then subjected to sodium dodecyl sulfate–12.5% polyacrylamide gel electrophoresis. The proteins were transferred to polyvinylidene difluoride membranes (Millipore, Bedford, MA) and then reacted with primary antibody and secondary horseradish peroxidase-conjugated antibody. The immunocomplexes were visualized with Super Signal West Femto substrate (Pierce, Rockford, IL) and detected by using an LAS-3000 image analyzer (Fujifilm, Tokyo, Japan). The distribution of VAPs in human organs was determined by using premade human tissue lysates (Protein medleys; Clonetech), which are aliquots of various organ lysates prepared from samples from several people, and liver tissues obtained during surgery after approval of the ethical committee of Kyushu University Graduate School of Medicine.

Real-time PCR. The HCV genomic RNA was determined by the method described previously (40). Total RNA was prepared from cells by using an RNeasy mini kit (Qiagen, Tokyo, Japan). First-strand cDNA was synthesized using an RNA LA PCR kit (Takara Bio, Inc., Shiga, Japan) and random primers. Expression of the appropriate gene was estimated by using platinum SYBR green quantitative PCR SuperMix UDG (Invitrogen, Carlsbad, CA) according to the manufacturer's protocol. Fluorescent signals were estimated by using an ABI Prism 7000 system (Applied Biosystems). The 5′ untranslated region of HCV and the glyceraldehyde-3-phosphate dehydrogenase (GAPDH) mRNA were amplified using primer pairs described previously (40). The amount of HCV genomic RNA was normalized with that of GAPDH mRNA.

Focus-forming assay. The viral RNA of the JFH1 strain was introduced into the Huh7OK1 cell line according to the method of Zhong et al. (51). The culture supernatant was collected at 7 days posttransfection and used as the infectious HCV particles. Huh7OK1 cells in DMEM containing 10% FCS were seeded at 5×10^4 cells per well into a 24-well plate 12 h before infection. The cells were infected with the JFH1 strain at a multiplicity of infection (MOI) of 0.05 and incubated at 37°C for 2 h. The medium was replaced with fresh DMEM containing 10% FCS and NEAA at 2 h postinfection. The cells were fixed with 4% paraformaldehyde at 96 h postinfection and permeabilized with PBS containing 0.2% Triton X-100. These fixed and permeabilized cells were stained with the anti-NS5A mouse monoclonal antibody and Alexa Fluor (AF) 488-conjugated antibody to mouse immunoglobulin G (Molecular Probes, Eugene, OR). Clusters of infected cells stained with the NS5A antibody were derived from a single infectious focus, and virus titers were represented as focus-forming units/ml.

Quantification of the HCV core protein by ELISA. The HCV core protein was quantified by using an Ortho HCV antigen enzyme-linked immunosorbent assay (ELISA) test (Ortho Clinical Diagnostics, Tokyo, Japan) according to the manufacturer's instructions. To determine the intracellular expression of core protein, Huh7OK1 cells were infected with the infectious HCV particles described above, lysed with the lysis buffer on ice, and applied to the ELISA after 100- to 10,000-fold dilution with PBS. Total protein was quantified by using a Micro BCA protein assay reagent kit (Pierce). The intracellular and extracellular levels of expression of the core protein were normalized by the total amount of protein.

Effect of the VAP expression on the cap-independent translational activity of the viral IRES. The cDNA fragment encoding a firefly luciferase was excised from a pGL3 basic plasmid (Promega, Madison, WI) and introduced into the downstream region of the *Renilla* luciferase gene of pRL-CMV (cytomegalovirus) (Promega). Then, the cDNA fragments encoding the internal ribosome entry site (IRES) of the HCV strains Con1 and JFH1 were introduced between the *Renilla* and firefly luciferase genes, and the resulting plasmids were designated pRL-CMV-HCVCon1 and pRL-CMV-HCVJFH1, respectively (see Fig. 4A). The IRES region of HCV was replaced with that of poliovirus (PV) or encephalomyocarditis virus (EMCV), and the plasmids designated pRL-CMV-PV and pRL-CMV-EMCV, respectively (see Fig. 4B). Each reporter plasmid was introduced into Huh7OK1 cells that had been transfected with the expression plasmid encoding FLAG-green fluorescent protein (GFP), FLAG–VAP-A, FLAG–VAP-B, or FLAG–VAP-C 24 h previously, and cells were harvested at 48 h posttransfection. Luciferase activities in cells were measured by using a dual-luciferase reporter assay system (Promega). The activity of firefly luciferase was normalized with that of *Renilla* luciferase and represented as relative luciferase activity (RLU).

Indirect immunofluorescence assay. The Huh 9-13 cells were cultured on glass slides and transfected with the expression plasmids encoding FLAG-tagged VAPs, P56S VAP mutants, or empty vector. The resulting cells were fixed at 72 h posttransfection with 4% paraformaldehyde in PBS at room temperature for 30 min. After being washed twice with PBS, cells were permeabilized for 20 min at room temperature with PBS containing 0.25% saponin and blocked with PBS containing 1% bovine serum albumin (BSA-PBS) for 60 min at room temperature. The cells were then incubated with BSA-PBS containing rabbit anti-FLAG and mouse anti-NS5A antibodies at 37°C for 60 min, washed three times with PBS containing 1% Tween 20 (PBS-T), and incubated with BSA-PBS containing AF 488-conjugated goat anti-rabbit immunoglobulin G and AF 594-conjugated goat anti-mouse antibodies at 37°C for 60 min. Finally, the cells were washed three times with PBS-T and observed with a FluoView FV1000 laser-scanning confocal microscope (Olympus, Tokyo, Japan).

RESULTS

VAP-C interacts with neither VAP-A nor VAP-B. The length of VAP-A was originally reported to be 242 amino acids but was recently corrected to 249 amino acids in the GenBank database due to the detection of 7 extra amino acids in the N terminus (Fig. 1A). VAP-C is a splicing variant of VAP-B that shares the N-terminal half of the MSP domain with VAP-B but lacks the coiled-coil motif and TM region (Fig. 1A). The region spanning residues 71 to 99 of VAP-C exhibits no homology to VAP-A and VAP-B, due to the frameshift. VAP-A and VAP-B form homo- or heterodimers via their TM domains, which is required for HCV replication (9, 44). To examine whether VAP-C is capable of interacting with VAP-A and VAP-B, FLAG-tagged VAP-A, -B, or -C was coexpressed with EE-tagged VAP-A or -B in 293T cells and was immunoprecipitated with the anti-FLAG antibody. Although EE-tagged VAP-A and VAP-B were coprecipitated with FLAG-tagged VAP-B and VAP-A, as reported previously, FLAG–VAP-C was precipitated with neither EE–VAP-A nor EE–VAP-B (Fig. 1B). These results indicate that VAP-C does not interact with VAP-A and VAP-B.

VAP-C binds to NS5B and interrupts the interaction of VAP-A and VAP-B with NS5B. VAP-A and VAP-B were identified as NS5A-binding proteins by yeast two-hybrid screening (9, 44). The coiled-coil domains of VAP-A and VAP-B were involved in the binding to NS5A, contributing to the efficiency of HCV replication (9, 44). However, VAP-C does not have the coiled-coil domain (Fig. 1A) and, therefore, VAP-C was expected not to interact with NS5A. To examine whether or not interaction between VAP-C and NS5A actually occurred, HA-tagged NS5A was coexpressed with FLAG-tagged VAP-A, -B, or -C in 293T cells and was immunoprecipitated with anti-HA antibody (Fig. 2). The results showed that the expression level of FLAG–VAP-C in the transfected cells was comparable to that of FLAG–VAP-A or FLAG–VAP-B (Fig. 2A, left). Although FLAG-tagged VAP-A and VAP-B were coprecipitated with HA-NS5A, no precipitation of FLAG–VAP-C with NS5A was detected (Fig. 2A, right), indicating that VAP-C does not interact with NS5A.

The RNA-dependent RNA polymerase NS5B was shown to interact with VAP-A through the MSP domain (44). The region spanning residues 1 to 70 of VAP-C is the same as the N-terminal-half region of the MSP domain of VAP-B and exhibits 77% homology to that of VAP-A (Fig. 1A). To exam-

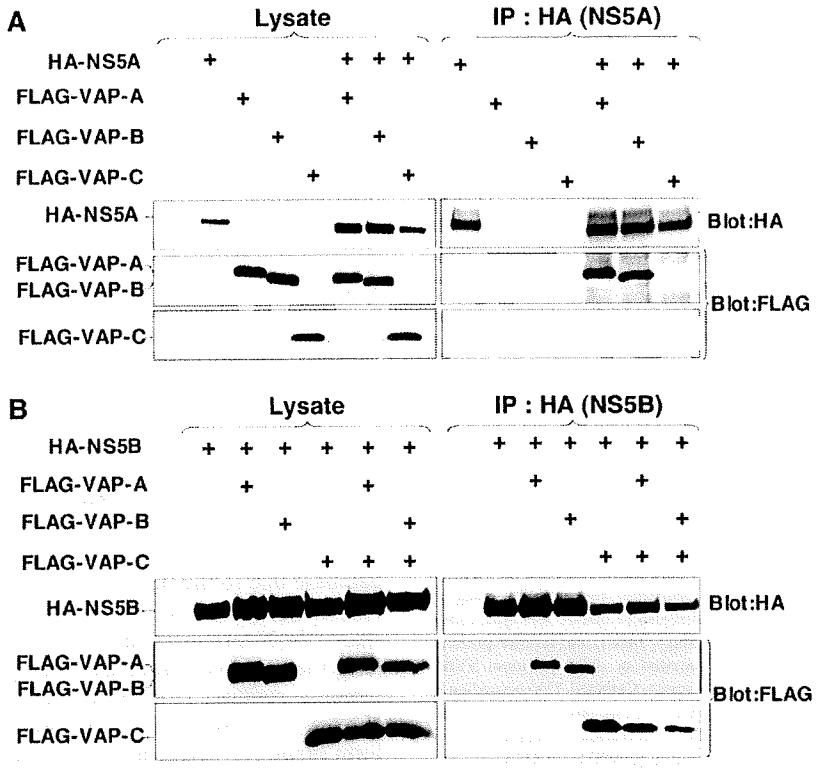

FIG. 2. VAP-C binds to NS5B but not NS5A and interrupts the interaction of VAP-A and VAP-B with NS5B. (A) The expression plasmids encoding NS5A or VAP proteins (1 μg each) were transfected into 293T cells after adjusting the total amounts of DNA to 2.0 μg with empty plasmid. HA-tagged NS5A was coexpressed with either FLAG-tagged VAP-A, VAP-B, or VAP-C in 293T cells and immunoprecipitated (IP) with anti-HA antibody, and the resulting precipitates were immunoblotted using anti-FLAG or anti-HA antibody. (B) The expression plasmids encoding NS5B or VAP proteins (1 μg each) were transfected into 293T cells after adjusting the total amounts of DNA to 3.0 μg with empty plasmid. HA-tagged NS5B was coexpressed with either FLAG-tagged VAP-A or VAP-B in the presence or absence of FLAG-tagged VAP-C in 293T cells and immunoprecipitated (IP) with anti-HA antibody, and the resulting precipitates were immunoblotted using anti-FLAG or anti-HA antibody. One percent of the lysate was used as an input control. The data in each panel are representative of the results of three independent experiments. +, present.

ine whether VAP-C is capable of interacting with NS5B, as are VAP-A and VAP-B, HA-NS5B was coexpressed with FLAG–VAP-A, FLAG–VAP-B, or FLAG–VAP-C in 293T cells and was immunoprecipitated with anti-HA antibody (Fig. 2B). Although substantial amounts of FLAG-tagged VAP-A, VAP-B, and VAP-C were coexpressed, and although all three were coprecipitated with HA-NS5B at comparable levels, the interaction of HA-NS5B with FLAG-tagged VAP-A or VAP-B was impaired by the coexpression of VAP-C, while FLAG–VAP-C was coprecipitated with HA-NS5B instead of FLAG-tagged VAP-A or VAP-B. These results suggest that VAP-C is capable of binding to NS5B and that the expression of VAP-C interrupts the interactions of NS5B with VAP-A and VAP-B.

Expression of VAP-C impairs the replication of HCV. VAP-A and VAP-B are known to support the replication of HCV RNA (2, 7). To examine the effect of VAP-C on the replication of HCV, FLAG–VAP-C was expressed in HCV replicon cells, Huh 9-13, in which a subgenomic HCV RNA of the genotype 1b strain Con1 was autonomously replicating. Huh 9-13 cells transfected with a plasmid encoding FLAG–VAP-C were harvested periodically up to 72 h posttransfection. The levels of replication of viral RNA and expression of NS5A were determined by real-time PCR and immunoblotting, respectively (Fig. 3). The expression of VAP-C reduced the intracellular RNA of the subgenomic HCV replicon in accordance with the incubation period after transfection with the expression plasmid of FLAG–VAP-C; the empty plasmid did not reduce the intracellular RNA (Fig. 3A). The expression of NS5A was gradually decreased and was undetectable at 72 h posttransfection, in contrast to the increase of VAP-C expression (Fig. 3B).

Next, to determine the effects of VAP-C expression on the replication of HCV, Huh 9-13 cells were transfected with 0 to 4 μg of the expression plasmid encoding VAP-A, VAP-B, or VAP-C and the replication of the subgenomic HCV RNA was determined at 48 h posttransfection. Although the HCV replicon cells transfected with 4 μg of a plasmid encoding FLAG–VAP-B exhibited enhancement of the RNA replication, those transfected with an equivalent amount of plasmid encoding FLAG–VAP-A or empty vector showed a slight reduction of HCV RNA replication. In contrast, the replicon cells transfected with a plasmid encoding FLAG–VAP-C exhibited a clear reduction of the HCV RNA replication in a dose-dependent manner (Fig. 3C). The expression of FLAG-tagged VAP-A, VAP-B, or VAP-C in the replicon cells was increased in correspondence with the amount of the transfected plasmid

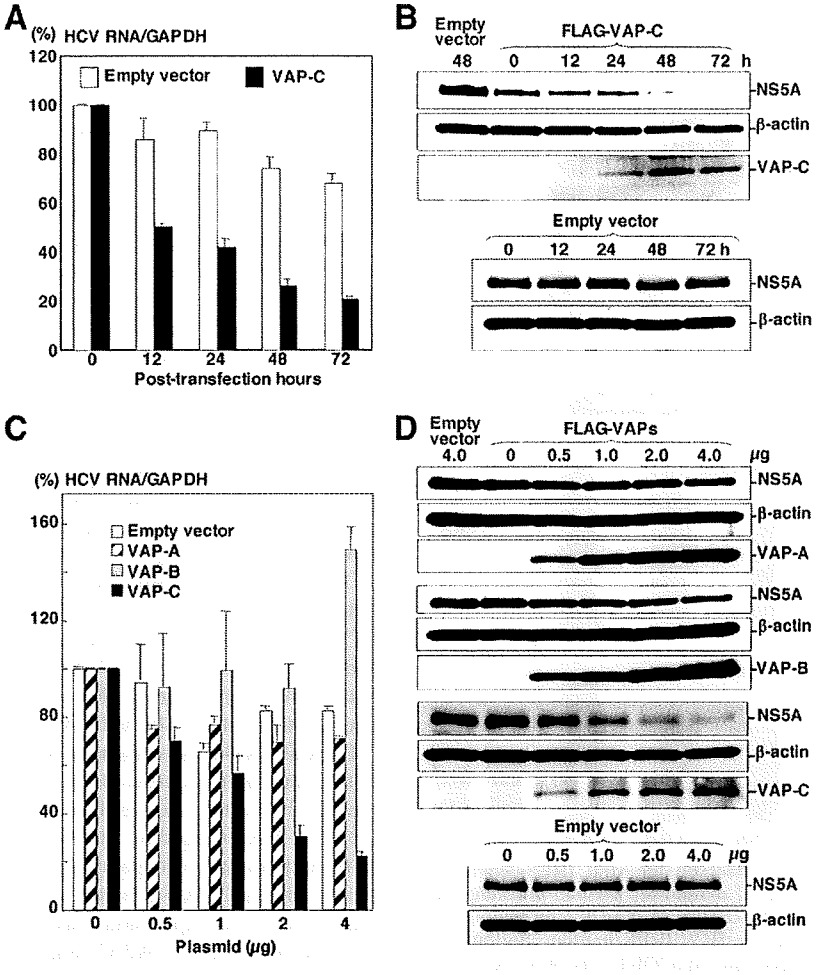

FIG. 3. Expression of VAP-C impairs the replication of HCV. (A) HCV replicon cells (Huh 9-13) were transfected with 4 μg of the expression plasmids encoding FLAG-tagged VAP-C or empty vector, and the level of intracellular HCV RNA was determined at 0, 12, 24, 48, or 72 h posttransfection by real-time PCR after normalization with GAPDH mRNA. The value of HCV RNA at 0 h posttransfection in the cell line transfected with the empty plasmid is represented as 100%. Data in this panel are shown as means ± standard deviations. (B) Huh 9-13 cells were transfected with 4 μg of the plasmid encoding FLAG-tagged VAP-C or empty plasmid, and the levels of expression of NS5A, β-actin, and VAP-C were determined at 0, 12, 24, 48, or 72 h posttransfection by immunoblotting using anti-NS5A, anti-β-actin, or anti-FLAG tag antibody. (C) Huh 9-13 cells were transfected with 0 to 4 μg of the plasmids encoding FLAG-tagged VAP-A, VAP-B, or VAP-C or empty vector, and the level of intracellular HCV RNA was determined at 72 h posttransfection as described for panel A. Data in this panel are shown as means ± standard deviations. (D) Huh 9-13 cells treated as described for panel C were harvested at 72 h posttransfection, and the levels of expression of NS5A, β-actin, VAP-A, VAP-B, and VAP-C were determined by immunoblotting. The data in each panel are representative of the results of three independent experiments.

(Fig. 3D), and the expression of NS5A was suppressed in accordance with the expression of FLAG–VAP-C, whereas the expression of FLAG–VAP-A and FLAG–VAP-B exhibited no effect on the expression of NS5A. These results suggest that the expression of VAP-C impairs the replication of HCV RNA.

VAP-C exhibits no effect on the IRES-dependent translation. The expression of VAP-C was shown to suppress the replication of the HCV RNA replication of the replicon cells. Next, to determine the effect of VAPs on the translation of HCV RNA, the reporter plasmid encoding the *Renilla* luciferase gene under the control of the CMV promoter and the firefly luciferase gene under the IRES of HCV, PV, or EMCV, in that order, was prepared as shown in Fig. 4. These reporter plasmids were introduced into Huh7OK1 cells 24 h after transfection of the expression plasmids encoding VAP-A, VAP-B, or VAP-C and harvested at 48 h posttransfection, and then the RLUs were determined. Although VAP-C exhibited a slight increase in the IRES-dependent translations of the HCV strains Con1 and JFH1, no significant effect of the expression of the VAPs on the HCV IRES-dependent translation was observed (Fig. 4A). Similarly, the expression of each of the VAPs in Huh7OK1 cells exhibited no significant effect on the IRES-dependent translation of PV or EMCV (Fig. 4B). These results indicate that the suppression of HCV RNA replication by the expression of

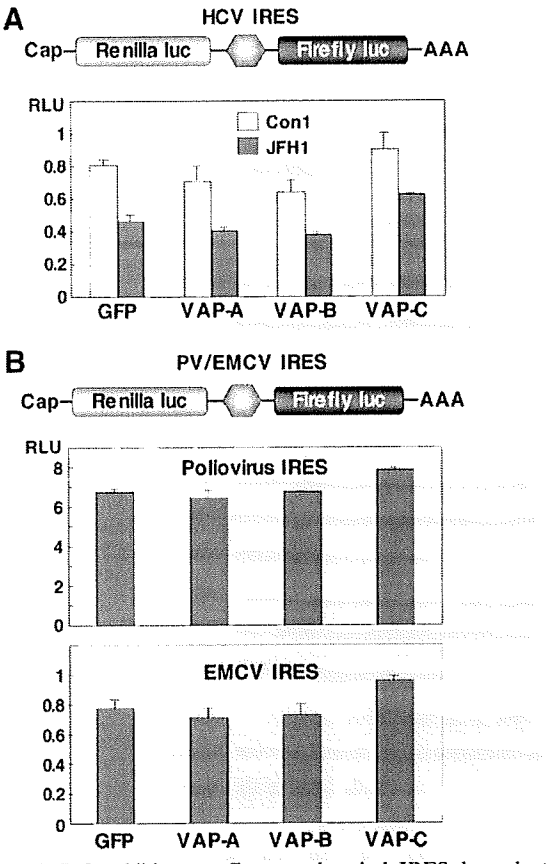

FIG. 4. VAP-C exhibits no effect on the viral IRES-dependent translation. (A) Top: structure of a reporter plasmid encoding the *Renilla* luciferase gene under the control of the CMV promoter and the firefly luciferase gene under the HCV IRES, in order. Bottom: the reporter plasmid was introduced into Huh7OK1 cells 24 h after transfection of the expression plasmids encoding VAP-A, VAP-B, or VAP-C, the cells harvested at 48 h posttransfection, and the RLUs determined after standardization with the expression of *Renilla* luciferase. (B) Top: structure of a reporter plasmid encoding the *Renilla* luciferase gene under the control of the CMV promoter and the firefly luciferase gene under the PV or EMCV IRES, in order. Bottom: each of the reporter plasmids was introduced into Huh7OK1 cells, and the RLU values were determined as described for panel A. Data in this figure are shown as the means ± standard deviations.

VAP-C was not due to the suppression of the IRES-dependent translation of the viral RNA genome.

VAP-C impairs HCV propagation. To examine the effect of VAP expression on HCV propagation, Huh7OK1 cells transfected with the expression plasmids encoding VAP-A, VAP-B, or VAP-C were infected with JFH1 virus, and the levels of production of the viral RNA, core protein, and infectious particles were determined at 96 h postinfection. The production of intracellular and extracellular viral RNA was increased up to 10 to 30 times and 2 to 3 times, respectively, by the expression of VAP-A or VAP-B whereas it was clearly decreased in a dose-dependent manner by the expression of VAP-C (Fig. 5A). Although the extracellular core protein was increased from 0.6 to 2.6 nmol/liter by the expression of VAP-A or VAP-B, as seen in the production of viral RNA, the intracellular core protein showed only a marginal increase (40 to 65 nmol/liter) (Fig. 5A). Although the reason for the discrepancy between the intracellular production of viral RNA and core protein is not known at the moment, some mechanisms other than RNA translation might be involved, because VAP expression exhibited no effect on the HCV IRES-dependent translation, as shown in Fig. 4A. In contrast to the enhancement of core protein production by the expression of VAP-A or VAP-B, the expression of VAP-C significantly reduced both the intracellular and extracellular expression of the core protein (Fig. 5A). Furthermore, the production of infectious particles in the culture supernatants of Huh7OK1 cells infected with JFH1 virus was slightly enhanced by the expression of VAP-A or VAP-B, whereas it was suppressed by the expression of VAP-C (Fig. 5A). To further confirm the effects of VAPs on the expression of HCV proteins, Huh7OK1 cells transfected with various amounts of the expression plasmids of VAP-A, VAP-B, or VAP-C and infected with the JFH1 virus were examined by immunoblotting (Fig. 5B). Although the expression of VAP-A or VAP-B exhibited no effect on NS5A expression, VAP-C expression clearly decreased the expression of NS5A in a dose-dependent manner. These results clearly indicate that the expression of VAP-C negatively regulates HCV propagation. Overexpression of VAP-C did not affect the endogenous expression of VAP-A or VAP-B (Fig. 5C), suggesting that suppression of HCV propagation by VAP-C is not due to the reduction of VAP-A or VAP-B expression.

Lack of VAP-C expression in human livers. VAP-C consists of the first 70 amino acid residues of VAP-B and the subtype-specific 29 amino acid residues derived from frameshift (Fig. 1A). The VAP-C-specific antibody generated by immunization with the peptide corresponding to the residues from 86 to 98 clearly detected VAP-C but neither VAP-A nor VAP-B in cells transfected with expression plasmids encoding FLAG-tagged VAP-A, VAP-B, or VAP-C (Fig. 6A). To determine the distribution of VAPs in human organs, the pool lysates of various organs prepared from several people were examined by immunoblotting (Fig. 6B). Expression of VAP-A was detected clearly in the kidney, lung, prostate, and liver; slightly in the duodenum, uterus, vagina, and bladder; and barely in the small intestine and stomach. VAP-B was detected clearly in the bladder, kidney, and prostate and slightly in the duodenum, small intestine, uterus, vagina, and liver. Expression of VAP-C was detected clearly in the stomach, uterus, kidney, and bladder; slightly in the duodenum, small intestine, and prostate; and barely detected in the vagina, lung, and liver. Several bands smaller than the expected size of VAP-C were observed in the stomach, duodenum, small intestine, uterus, vagina, prostate, and bladder. Because the main target of HCV replication is thought to be the liver, we next examined the expression of VAPs in individual human liver samples. VAP-A and VAP-B were clearly detected in the liver tissues obtained from chronic hepatitis C patients and a healthy donor, but no expression of VAP-C was detected (Fig. 6C). These results suggest that the expression of VAP-C may participate in the determination of tissue tropism of HCV propagation.

Substitution of Ser for Pro^{56} in VAPs leads to suppression of HCV replication. A single mutation of Pro^{56} to Ser (P56S) of VAP-B has been reported to be highly associated with amyotrophic lateral sclerosis (ALS), and the P56S mutation of VAP-B but not of VAP-A has been shown to induce large

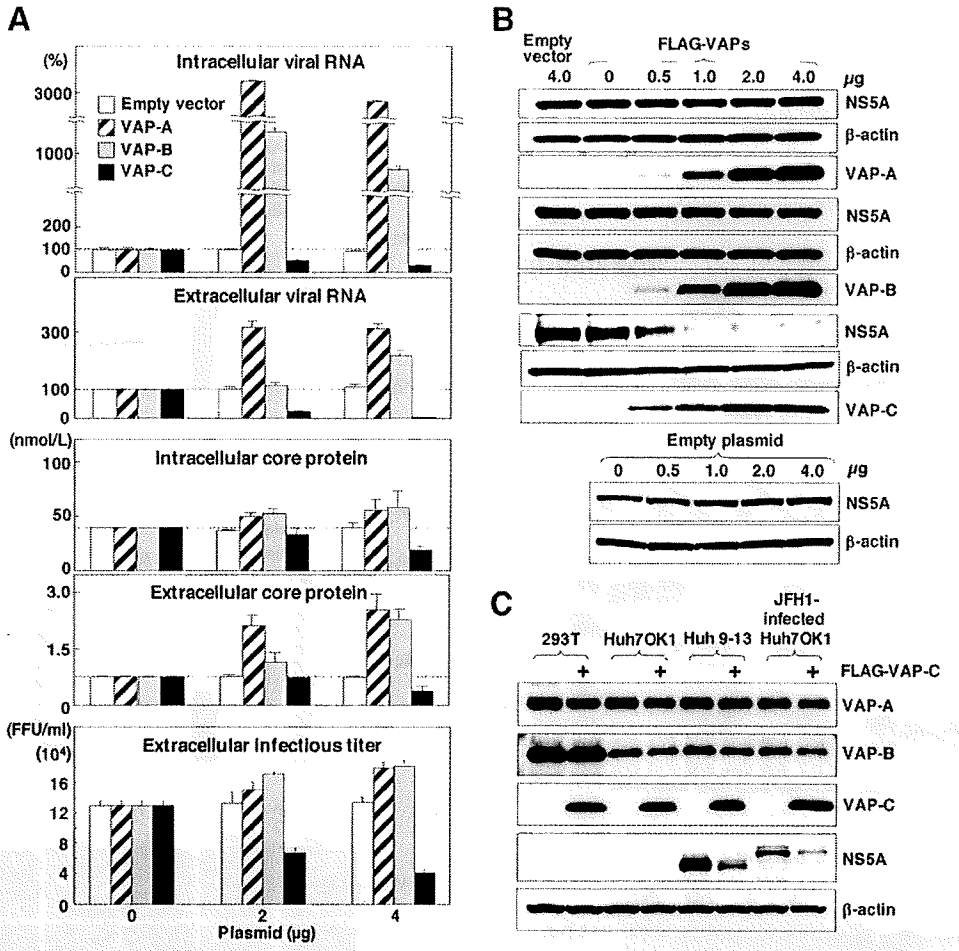

FIG. 5. VAP-C impairs HCV propagation but does not affect endogenous expression of VAP-A or VAP-B. Huh7OK1 cells transfected with 0 to 4 μg of plasmid encoding the FLAG-tagged VAP-A, VAP-B, or VAP-C or empty vector were infected with strain JFH1 at an MOI of 0.05 at 14 h posttransfection and then harvested at 96 h postinfection. (A) The intracellular and extracellular expression levels of viral RNA (top) and core protein (middle) were determined by real-time PCR and ELISA, respectively. Infectious viral titers in the culture supernatants were determined by focus-forming assay (bottom). Data in this panel are shown as the means ± standard deviations. (B) The expression levels of NS5A, β-actin, VAP-A, VAP-B, and VAP-C were determined by immunoblotting using anti-NS5A, anti-β-actin, or anti-FLAG tag antibody. (C) The embryonic kidney cell line (293T), the cured hepatoma cell line (Huh7OK1), and the replicon cell line (Huh 9-13) were transfected with 2 μg of the plasmid encoding FLAG-tagged VAP-C (+) or empty plasmid. In the case of the infected cells, Huh7OK1 cells were infected with strain JFH1 at an MOI of 0.05, reseeded onto the tissue culture plate at 96 h postinfection, and then transfected with 2 μg of the plasmids. These cells were harvested at 36 h posttransfection and examined by immunoblotting using antibodies to VAP-A, VAP-B, FLAG, NS5A, and β-actin. The data in each panel are representative of the results of three independent experiments.

aggregations of ER in culture cells and to sequester the wild-type protein into ubiquitinated inclusions (29, 37). To examine the effects on the replication of HCV of the P56S mutation in VAPs, FLAG-tagged VAP mutants were expressed in the HCV replicon cells. RNA replication of the subgenomic replicon in Huh 9-13 cells was impaired by the expression of each of the mutant VAPs (Fig. 7A, left). The expression of NS5A in the replicon cells was decreased by the expression of the mutant VAPs in a dose-dependent manner (Fig. 7A, right). Next, to examine the effect of the expression of the P56S VAP mutants on HCV propagation, Huh7OK1 cells expressing the FLAG-tagged VAP mutants were infected with JFH1 virus. The production of intracellular and extracellular viral RNA at 96 h postinfection was decreased by the expression of the P56S mutation in VAPs (Fig. 7B). Although the results of a previous study indicated that the expression of the P56S mutant of VAP-B but not that of VAP-A induced a large aggregation of ER in hamster ovary cell line CHO (37), the P56S mutants of VAP-A and VAP-B but not that of VAP-C exhibited accumulation of membranous aggregates in Huh 9-13 cells (Fig. 7C). These results indicate that the P56S mutation in both VAP-B and VAP-A induces aggregation of ER in human hepatoma cells, which in turn leads to the suppression of HCV propagation.

DISCUSSION

The replication of HCV has been shown to require several host proteins, including VAP-A/VAP-B (6, 9, 44), FBL2 (46), FKBP8 (34), hB-ind1 (40), Hsp90 (28, 34, 45), and cyclophilins

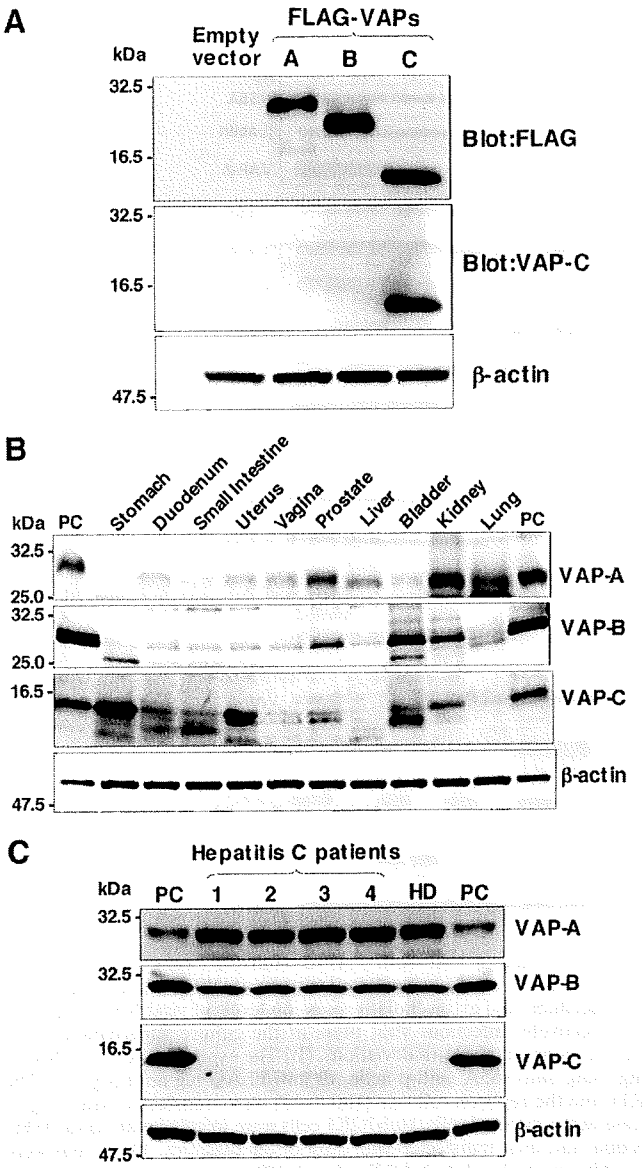

FIG. 6. Distribution of VAPs in human tissues. (A) Anti-VAP-C antibody specifically recognizes VAP-C. Human embryonic kidney 293T cells transfected with expression plasmid encoding FLAG-tagged VAP-A, VAP-B, or VAP-C or empty vector were harvested at 48 h posttransfection and examined by immunoblotting using anti-FLAG tag, anti-VAP-C, and anti-β-actin antibodies. (B) The premade human tissue lysates "Protein medleys" (20 μg each; Clonetech) were examined by immunoblotting using antibodies against VAP-A, VAP-B, VAP-C, or β-actin. (C) Expression of VAP family proteins in human liver tissues. Liver samples obtained from four hepatitis C patients (1 to 4) and one healthy donor (HD) were examined by immunoblotting as described above. The data in each panel are representative of the results of three independent experiments. PC indicates 293T cells transfected with expression plasmid encoding VAP-A, VAP-B, and VAP-C.

(15, 48). VAP-A has been detected in a detergent-resistant membrane fraction that was shown to be capable of replicating HCV RNA in vitro, and the interaction of VAP-A with NS5A is required for the efficient replication of HCV genomic RNA

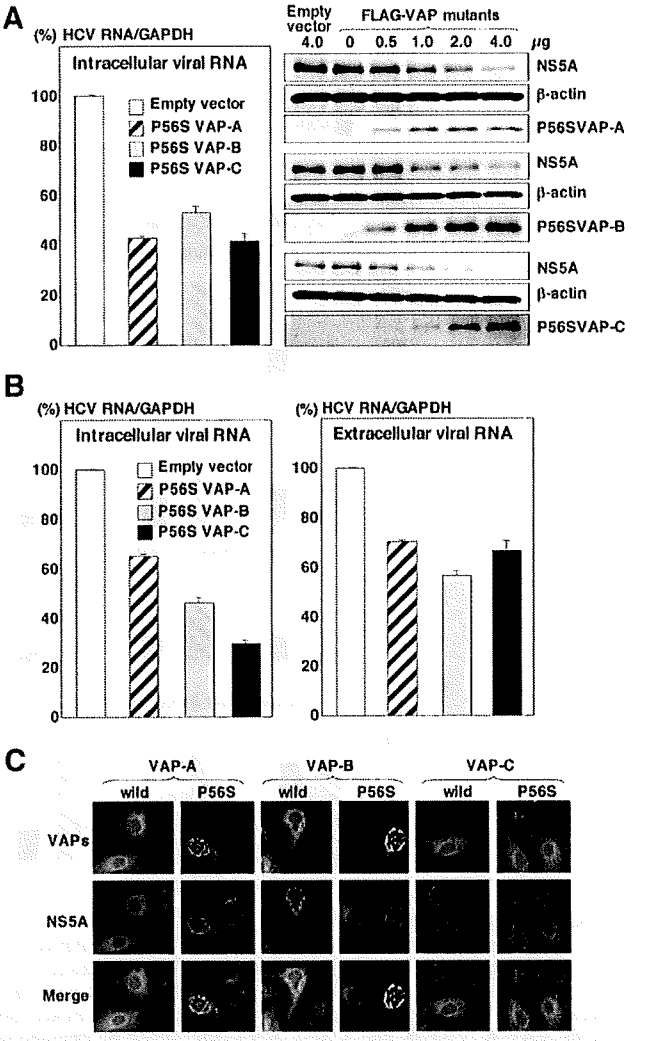

FIG. 7. Substitution of Ser for Pro[56] in VAPs leads to suppression of HCV replication. (A) Left: Huh 9-13 cells were transfected with 4 μg of the expression plasmids encoding FLAG-tagged P56S VAP mutants or empty vector, and the level of intracellular HCV RNA was determined at 72 h posttransfection by real-time PCR after normalization with GAPDH mRNA. The value for HCV RNA at 0 h posttransfection in the cell line transfected with the empty plasmid is represented as 100%. Data in this panel are shown as the means ± standard deviations. Right: Huh 9-13 cells were transfected with 0 to 4 μg of the FLAG-tagged P56S VAP mutant plasmids or empty vector, and the levels of expression of NS5A, β-actin, and the mutant VAPs were determined by immunoblotting at 72 h posttransfection. The data in each panel are representative of the results of three independent experiments. (B) Huh7OK1 cells transfected with 4 μg of the expression plasmids encoding FLAG-tagged P56S VAP mutants or empty vector were infected with strain JFH1 at an MOI of 0.05 at 14 h posttransfection, and the intracellular (left) and extracellular (right) expression levels of viral RNA were determined by real-time PCR after normalization with GAPDH mRNA at 96 h postinfection. Data in this panel are shown as the means ± standard deviations. (C) Levels of expression of wild-type VAPs, P56S mutant VAPs, and NS5A in Huh 9-13 cells at 72 h after transfection with the expression plasmids encoding FLAG-tagged VAPs or P56S VAP mutants were determined by immunofluorescent assay. The data in each panel are representative of the results of three independent experiments.

(2, 7) and is modulated by the phosphorylation of NS5A (4, 6). VAP-B also participates in HCV replication through the formation of homo- and/or heterodimers with VAP-A (9). VAP-A and VAP-B form hetero- and homodimers through their TM regions and interact with NS5A and NS5B through the coiled-coil domain and MSP domain, respectively (9, 44). VAP-C is a splicing variant of VAP-B, consisting of the N-terminal half of VAP-B and the subtype-specific amino acid residues generated by the frameshift. However, the biological significance of VAP-C in the life cycle of HCV has not been determined. In this study, we have demonstrated that VAP-C is capable of binding to HCV NS5B but not to NS5A, VAP-A, and VAP-B due to the lack of the coiled-coil and TM regions. The expression of VAP-C inhibited the interaction of VAP-A and VAP-B with NS5B, impaired the RNA replication and particle formation of HCV, and was barely detected in human liver cells. These results suggest that VAP-C acts as a negative regulator for HCV propagation and is partly involved in the determination of the tissue specificity of HCV replication.

Overexpression of VAP-A but not of VAP-B inhibited the incorporation of the vesicular stomatitis virus (VSV) envelope glycoprotein G (VSV-G) into ER vesicles in CHO cells, resulting in impairment of membrane protein transport from the ER to the Golgi apparatus (37). VAP-B was shown to be involved in the unfolded protein response, which is an ER reaction to suppress the accumulation of misfolded proteins, and the expression of the P56S VAP-B mutant was suggested to nullify the unfolded protein response induced by VAP-B, to produce a large aggregation of ER, and to be involved in the development of ALS (17, 37). These data suggest that VAP-A and VAP-B possess different physiological functions; however, the contributions of the proteins to the life cycle of HCV have not been characterized. The expression of VAP-B but not of VAP-A resulted in an enhancement of the replication of the subgenomic HCV RNA of the genotype 1b strain Con1, whereas the expression of either VAP-A or VAP-B clearly enhanced viral RNA replication in cells infected with the genotype 2a strain JFH1 virus, suggesting that the contributions of VAP-A and VAP-B to viral RNA replication might differ among the genotypes of HCV. The expression of VAP-B or VAP-A enhanced RNA replication in the HCV replicon cells and the secretion of viral RNA, core protein, and infectious particles into the culture supernatants of Huh7OK1 cells infected with JFH1 virus, whereas the expression of these proteins had no effect on the expression of NS5A or on IRES-dependent translation. Thus, further studies will be needed to clarify the molecular mechanisms underlying the posttranslational enhancement of HCV production by the expression of VAP-A and VAP-B. In contrast to the expression of VAP-A and VAP-B, the expression of VAP-C clearly suppressed the RNA replication of both the genotype 1b RNA replicon cells and the genotype 2a strain JFH1 virus, by which both the expression of the viral proteins and the viral particle production were drastically impaired. Furthermore, the expression of the P56S mutants of VAP-A and VAP-B reduced RNA replication in HCV replicon cells and propagation of the JFH1 virus, probably due to the induction of aggregation of the ER. The reason why ER aggregation was induced by the expression of the P56S VAP-A mutant in Huh7 cells but not in CHO cells (17, 37) is not known at the moment.

The phosphorylation state of NS5A was suggested to control the interaction between VAP-A and NS5A and the replication efficiency of HCV RNA (6). Introduction of the adaptive mutations originally identified in the genotype 1b strain Con1 into NS5A of genotype 1a suppressed the hyperphosphorylation of NS5A, potentiated interaction with VAP-A, and enhanced the RNA replication (6). However, we have previously shown that NS5A of genotype 1a could bind to VAP-A and VAP-B at a level similar to that of genotype 1b despite the adaptive mutations (9). In this study, overexpression of each of the VAP proteins exhibited no effect on the mobility of NS5A in sodium dodecyl sulfate-polyacrylamide gel electrophoresis (Fig. 3 and 5), suggesting that there is no correlation between the VAP-dependent regulation of HCV propagation and the phosphorylation state of NS5A.

FKBP8 exhibits peptidyl prolyl *cis-trans* isomerase activity and interacts with NS5A and Hsp90 through the tetratricopeptide repeat (TPR) domain, and these interactions are suggested to be involved in the correct folding of the HCV replication complex (34). Treatment of cells with inhibitors of the ATPase activity of Hsp90, such as geldanamycin and its derivatives, impairs the RNA replication and particle production of HCV (28, 34, 45). The MSP domain of VAP-A was shown to interact with the TPR1 protein, which has a TPR domain and forms the chaperone complex with Hsp90 (22). Knockdown of the TPR1 protein or treatment with Hsp90 inhibitors in mammalian cells has been shown to inhibit the transport of VSV-G, leading to accumulation of the glycoprotein in the Golgi apparatus (22). The VAP-A- or VAP-B-induced enhancement of virus production might be attributable to the recruitment of Hsp90 into the replication complex through the interaction with the MSP domain.

VAP-A is well known to interact through the MSP domain with a number of mammalian and yeast proteins sharing the FFAT motif, including OSBPs, ORPs (20), and CERT (10, 19), and to be involved in the regulation of biosynthesis or trafficking of sterols and lipids. HCV replication and infection have been shown to be regulated by lipid components and to be capable of being inhibited by treatment with several inhibitors targeting lipid biosynthesis (14, 18). The intracellular membranous web structure observed in HCV replicon cells was shown to be resistant to detergent treatment, suggesting that the lipid raft-like structure abundant in cholesterol and sphingolipid is generated by the replication of HCV RNA (2, 24). Therefore, it might be feasible to speculate that VAP-A and VAP-B are involved in the construction of the HCV replication complex consisting of viral proteins and host cellular lipid components and that VAP-C interrupts the VAP-A and VAP-B functions and negatively regulates HCV propagation. Although the molecular mechanisms and the biological significance remain to be clarified, the MSP domain of VAP proteins was processed in human leukocytes and secreted into human serum (43). Further studies are needed to clarify the biogenesis and biological functions of the truncated VAP proteins in the replication of HCV.

In summary, we have shown that VAP-C is capable of suppressing the RNA replication and particle production of HCV by inhibiting the binding of VAP-A and VAP-B to NS5B through the N-terminal half of its MSP domain. The clear suppression of HCV propagation by the expression of VAP-C

further suggests the possibility of developing a novel therapeutic measure to eliminate HCV by the exogenous expression of VAP-C in the hepatocytes of chronic hepatitis C patients.

ACKNOWLEDGMENTS

We thank H. Murase for her secretarial work. We also thank R. Bartenschlager and T. Wakita for providing cell lines and plasmids.

This work was supported in part by grants-in-aid from the Ministry of Health, Labor, and Welfare; the Ministry of Education, Culture, Sports, Science, and Technology; the Global Center of Excellence Program; and the Foundation for Biomedical Research and Innovation.

REFERENCES

1. **Abe, T., Y. Kaname, I. Hamamoto, Y. Tsuda, X. Wen, S. Taguwa, K. Moriishi, O. Takeuchi, T. Kawai, T. Kanto, N. Hayashi, S. Akira, and Y. Matsuura.** 2007. Hepatitis C Virus nonstructural protein 5A modulates Toll-like receptor-MyD88-dependent signaling pathway in the macrophage cell lines. J. Virol. **81**:8953–8966.
2. **Aizaki, H., K. J. Lee, V. M. Sung, H. Ishiko, and M. M. Lai.** 2004. Characterization of the hepatitis C virus RNA replication complex associated with lipid rafts. Virology **324**:450–461.
3. **Behrens, S. E., L. Tomei, and R. De Francesco.** 1996. Identification and properties of the RNA-dependent RNA polymerase of hepatitis C virus. EMBO J. **15**:12–22.
4. **Blight, K. J., A. A. Kolykhalov, and C. M. Rice.** 2000. Efficient initiation of HCV RNA replication in cell culture. Science **290**:1972–1974.
5. **Egger, D., B. Wolk, R. Gosert, L. Bianchi, H. E. Blum, D. Moradpour, and K. Bienz.** 2002. Expression of hepatitis C virus proteins induces distinct membrane alterations including a candidate viral replication complex. J. Virol. **76**:5974–5984.
6. **Evans, M. J., C. M. Rice, and S. P. Goff.** 2004. Phosphorylation of hepatitis C virus nonstructural protein 5A modulates its protein interactions and viral RNA replication. Proc. Natl. Acad. Sci. USA **101**:13038–13043.
7. **Gao, L., H. Aizaki, J.-W. He, and M. M. C. Lai.** 2004. Interactions between viral nonstructural proteins and host protein hVAP-33 mediate the formation of hepatitis C virus RNA replication complex on lipid raft. J. Virol. **78**:3480–3488.
8. **Grakoui, A., D. W. McCourt, C. Wychowski, S. M. Feinstone, and C. M. Rice.** 1993. Characterization of the hepatitis C virus-encoded serine proteinase: determination of proteinase-dependent polyprotein cleavage sites. J. Virol. **67**:2832–2843.
9. **Hamamoto, I., Y. Nishimura, T. Okamoto, H. Aizaki, M. Liu, Y. Mori, T. Abe, T. Suzuki, M. M. Lai, T. Miyamura, K. Moriishi, and Y. Matsuura.** 2005. Human VAP-B is involved in hepatitis C virus replication through interaction with NS5A and NS5B. J. Virol. **79**:13473–13482.
10. **Hanada, K., K. Kumagai, S. Yasuda, Y. Miura, M. Kawano, M. Fukasawa, and M. Nishijima.** 2003. Molecular machinery for non-vesicular trafficking of ceramide. Nature **426**:803–809.
11. **Ho, S. N., H. D. Hunt, R. M. Horton, J. K. Pullen, and L. R. Pease.** 1989. Site-directed mutagenesis by overlap extension using the polymerase chain reaction. Gene **77**:51–59.
12. **Hoofnagle, J. H.** 2002. Course and outcome of hepatitis C. Hepatology **36**:S21–S29.
13. **Huang, D. C., S. Cory, and A. Strasser.** 1997. Bcl-2, Bcl-XL and adenovirus protein E1B19kD are functionally equivalent in their ability to inhibit cell death. Oncogene **14**:405–414.
14. **Ikeda, M., K. Abe, M. Yamada, H. Dansako, K. Naka, and N. Kato.** 2006. Different anti-HCV profiles of statins and their potential for combination therapy with interferon. Hepatology **44**:117–125.
15. **Inoue, K., T. Umehara, U. T. Ruegg, F. Yasui, T. Watanabe, H. Yasuda, J. M. Dumont, P. Scalfaro, M. Yoshiba, and M. Kohara.** 2007. Evaluation of a cyclophilin inhibitor in hepatitis C virus-infected chimeric mice in vivo. Hepatology **45**:921–928.
16. **Kaiser, S. E., J. H. Brickner, A. R. Reilein, T. D. Fenn, P. Walter, and A. T. Brunger.** 2005. Structural basis of FFAT motif-mediated ER targeting. Structure **13**:1035–1045.
17. **Kanekura, K., I. Nishimoto, S. Aiso, and M. Matsuoka.** 2006. Characterization of amyotrophic lateral sclerosis-linked P56S mutation of vesicle-associated membrane protein-associated protein B (VAPB/ALS8). J. Biol. Chem. **281**:30223–30233.
18. **Kapadia, S. B., and F. V. Chisari.** 2005. Hepatitis C virus RNA replication is regulated by host geranylgeranylation and fatty acids. Proc. Natl. Acad. Sci. USA **102**:2561–2566.
19. **Kawano, M., K. Kumagai, M. Nishijima, and K. Hanada.** 2006. Efficient trafficking of ceramide from the endoplasmic reticulum to the Golgi apparatus requires a VAMP-associated protein-interacting FFAT motif of CERT. J. Biol. Chem. **281**:30279–30288.
20. **Loewen, C. J., A. Roy, and T. P. Levine.** 2003. A conserved ER targeting motif in three families of lipid binding proteins and in Opi1p binds VAP. EMBO J. **22**:2025–2035.
21. **Lohmann, V., F. Korner, J. Koch, U. Herian, L. Theilmann, and R. Bartenschlager.** 1999. Replication of subgenomic hepatitis C virus RNAs in a hepatoma cell line. Science **285**:110–113.
22. **Lotz, G. P., A. Brychzy, S. Heinz, and W. M. Obermann.** 2008. A novel HSP90 chaperone complex regulates intracellular vesicle transport. J. Cell Sci. **121**:717–723.
23. **McLauchlan, J., M. K. Lemberg, G. Hope, and B. Martoglio.** 2002. Intramembrane proteolysis promotes trafficking of hepatitis C virus core protein to lipid droplets. EMBO J. **21**:3980–3988.
24. **Miyanari, Y., M. Hijikata, M. Yamaji, M. Hosaka, H. Takahashi, and K. Shimotohno.** 2003. Hepatitis C virus non-structural proteins in the probable membranous compartment function in viral genome replication. J. Biol. Chem. **278**:50301–50308.
25. **Moriishi, K., and Y. Matsuura.** 2007. Host factors involved in the replication of hepatitis C virus. Rev. Med. Virol. **17**:343–354.
26. **Moriishi, K., and Y. Matsuura.** 2003. Mechanisms of hepatitis C virus infection. Antivir. Chem. Chemother. **14**:285–297.
27. **Moriishi, K., T. Okabayashi, K. Nakai, K. Moriya, K. Koike, S. Murata, T. Chiba, K. Tanaka, R. Suzuki, T. Suzuki, T. Miyamura, and Y. Matsuura.** 2003. Proteasome activator PA28gamma-dependent nuclear retention and degradation of hepatitis C virus core protein. J. Virol. **77**:10237–10249.
28. **Nakagawa, S., T. Umehara, C. Matsuda, S. Kuge, M. Sudoh, and M. Kohara.** 2007. Hsp90 inhibitors suppress HCV replication in replicon cells and humanized liver mice. Biochem. Biophys. Res. Commun. **353**:882–888.
29. **Nishimura, A. L., M. Mitne-Neto, H. C. Silva, A. Richieri-Costa, S. Middleton, D. Cascio, F. Kok, J. R. Oliveira, T. Gillingwater, J. Webb, P. Skehel, and M. Zatz.** 2004. A mutation in the vesicle-trafficking protein VAPB causes late-onset spinal muscular atrophy and amyotrophic lateral sclerosis. Am. J. Hum. Genet. **75**:822–831.
30. **Nishimura, Y., M. Hayashi, H. Inada, and T. Tanaka.** 1999. Molecular cloning and characterization of mammalian homologues of vesicle-associated membrane protein-associated (VAMP-associated) proteins. Biochem. Biophys. Res. Commun. **254**:21–26.
31. **Niwa, H., K. Yamamura, and J. Miyazaki.** 1991. Efficient selection for high-expression transfectants with a novel eukaryotic vector. Gene **108**:193–199.
32. **Okamoto, K., Y. Mori, Y. Komoda, T. Okamoto, M. Okochi, M. Takeda, T. Suzuki, K. Moriishi, and Y. Matsuura.** 2008. Intramembrane processing by signal peptide peptidase regulates the membrane localization of hepatitis C virus core protein and viral propagation. J. Virol. **82**:8349–8361.
33. **Okamoto, K., K. Moriishi, T. Miyamura, and Y. Matsuura.** 2004. Intramembrane proteolysis and endoplasmic reticulum retention of hepatitis C virus core protein. J. Virol. **78**:6370–6380.
34. **Okamoto, T., Y. Nishimura, T. Ichimura, K. Suzuki, T. Miyamura, T. Suzuki, K. Moriishi, and Y. Matsuura.** 2006. Hepatitis C virus RNA replication is regulated by FKBP8 and Hsp90. EMBO J. **25**:5015–5025.
35. **Okamoto, T., H. Omori, Y. Kaname, T. Abe, Y. Nishimura, T. Suzuki, T. Miyamura, T. Yoshimori, K. Moriishi, and Y. Matsuura.** 2008. A single-amino-acid mutation in hepatitis C virus NS5A disrupting FKBP8 interaction impairs viral replication. J. Virol. **82**:3480–3489.
36. **Pennetta, G., P. R. Hiesinger, R. Fabian-Fine, I. A. Meinertzhagen, and H. J. Bellen.** 2002. Drosophila VAP-33A directs bouton formation at neuromuscular junctions in a dosage-dependent manner. Neuron **35**:291–306.
37. **Prosser, D. C., D. Tran, P. Y. Gougeon, C. Verly, and J. K. Ngsee.** 2008. FFAT rescues VAPA-mediated inhibition of ER-to-Golgi transport and VAPB-mediated ER aggregation. J. Cell Sci. **121**:3052–3061.
38. **Skehel, P. A., R. Fabian-Fine, and E. R. Kandel.** 2000. Mouse VAP33 is associated with the endoplasmic reticulum and microtubules. Proc. Natl. Acad. Sci. USA **97**:1101–1106.
39. **Skehel, P. A., K. C. Martin, E. R. Kandel, and D. Bartsch.** 1995. A VAMP-binding protein from *Aplysia* required for neurotransmitter release. Science **269**:1580–1583.
40. **Taguwa, S., T. Okamoto, T. Abe, Y. Mori, T. Suzuki, K. Moriishi, and Y. Matsuura.** 2008. Human butyrate-induced transcript 1 interacts with hepatitis C virus NS5A and regulates viral replication. J. Virol. **82**:2631–2641.
41. **Tellinghuisen, T. L., J. Marcotrigiano, and C. M. Rice.** 2005. Structure of the zinc-binding domain of an essential component of the hepatitis C virus replicase. Nature **435**:374–379.
42. **Tomei, L., C. Failla, E. Santolini, R. De Francesco, and N. La Monica.** 1993. NS3 is a serine protease required for processing of hepatitis C virus polyprotein. J. Virol. **67**:4017–4026.
43. **Tsuda, H., S. M. Han, Y. Yang, C. Tong, Y. Q. Lin, K. Mohan, C. Haueter, A. Zoghbi, Y. Harati, J. Kwan, M. A. Miller, and H. J. Bellen.** 2008. The amyotrophic lateral sclerosis 8 protein VAPB is cleaved, secreted, and acts as a ligand for Eph receptors. Cell **133**:963–977.
44. **Tu, H., L. Gao, S. T. Shi, D. R. Taylor, T. Yang, A. K. Mircheff, Y. Wen, A. E. Gorbalenya, S. B. Hwang, and M. M. Lai.** 1999. Hepatitis C virus RNA polymerase and NS5A complex with a SNARE-like protein. Virology **263**: 30–41.

45. **Ujino, S., S. Yamaguchi, K. Shimotohno, and H. Takaku.** 2009. Heat-shock protein 90 is essential for stabilization of the hepatitis C virus non-structural protein NS3. J. Biol. Chem. **284**:6841–6846.
46. **Wang, C., M. Gale, Jr., B. C. Keller, H. Huang, M. S. Brown, J. L. Goldstein, and J. Ye.** 2005. Identification of FBL2 as a geranylgeranylated cellular protein required for hepatitis C virus RNA replication. Mol. Cell **18**:425–434.
47. **Wasley, A., and M. J. Alter.** 2000. Epidemiology of hepatitis C: geographic differences and temporal trends. Semin. Liver Dis. **20**:1–16.
48. **Watashi, K., N. Ishii, M. Hijikata, D. Inoue, T. Murata, Y. Miyanari, and K. Shimotohno.** 2005. Cyclophilin B is a functional regulator of hepatitis C virus RNA polymerase. Mol. Cell **19**:111–122.
49. **Weir, M. L., A. Klip, and W. S. Trimble.** 1998. Identification of a human homologue of the vesicle-associated membrane protein (VAMP)-associated protein of 33 kDa (VAP-33): a broadly expressed protein that binds to VAMP. Biochem. J. **333**:247–251.
50. **Weir, M. L., H. Xie, A. Klip, and W. S. Trimble.** 2001. VAP-A binds promiscuously to both v- and tSNAREs. Biochem. Biophys. Res. Commun. **286**:616–621.
51. **Zhong, J., P. Gastaminza, G. Cheng, S. Kapadia, T. Kato, D. R. Burton, S. F. Wieland, S. L. Uprichard, T. Wakita, and F. V. Chisari.** 2005. Robust hepatitis C virus infection in vitro. Proc. Natl. Acad. Sci. USA **102**:9294–9299.

Proteomics Analysis of Mitochondrial Proteins Reveals Overexpression of a Mitochondrial Protein Chaperon, Prohibitin, in Cells Expressing Hepatitis C Virus Core Protein

Takeya Tsutsumi,[1] Mami Matsuda,[2] Hideki Aizaki,[2] Kyoji Moriya,[1] Hideyuki Miyoshi,[1] Hajime Fujie,[1] Yoshizumi Shintani,[1] Hiroshi Yotsuyanagi,[1] Tatsuo Miyamura,[2] Tetsuro Suzuki,[2] and Kazuhiko Koike[1]

The hepatitis C virus (HCV) core protein is involved in viral pathogenesis such as oxidative stress induction and lipid metabolism disturbance, and is primarily located in the cytoplasm and endoplasmic reticulum in association with lipid droplets as well as in the mitochondria. To clarify the impact of the core protein on mitochondria, we analyzed the expression pattern of mitochondrial proteins in core protein-expressing cells by two-dimensional polyacrylamide gel electrophoresis. Several proteins related to the mitochondrial respiratory chain or protein chaperons were identified by mass spectrometry. Among the identified proteins with consistently different expressions, prohibitin, a mitochondrial protein chaperon, was up-regulated not only in core-expressing cells but also in full-genomic replicon cells and livers of core-gene transgenic mice. The stability of prohibitin was increased through interaction with the core protein. Further analysis demonstrated that interaction of prohibitin with mitochondrial DNA-encoded subunits of cytochrome c oxidase (COX) was disturbed by the core protein, resulting in a significant decrease in COX activity. *Conclusion:* The HCV core protein affects the steady-state levels of a subset of mitochondrial proteins including prohibitin, which may lead to an impaired function of the mitochondrial respiratory chain with the overproduction of oxidative stress. (HEPATOLOGY 2009;50:378-386.)

The hepatitis C virus (HCV) is a causative agent of chronic hepatitis, which often leads to cirrhosis and, eventually, to the development of hepatocellular carcinoma (HCC). However, the mechanism of hepatocarcinogenesis in HCV infection is not yet fully elucidated. The HCV core protein forms the viral nucleocapsid protein and has various properties that modulate cellular processes in numerous ways. The core protein binds to cellular proteins, suppresses or enhances apoptosis, and modulates the transcription of some host genes.[1] In addition, transgenic mice expressing the core protein develop HCC,[2-4] indicating a direct contribution of the core protein to the pathogenesis of hepatitis C.

The core protein is mostly localized to the endoplasmic reticulum (ER), but we and other groups have shown its localization to the mitochondria in cultured cells and transgenic mice.[2,5,6] In addition, the double structure of mitochondrial membranes is disrupted in hepatocytes of core-gene transgenic mice.[2-4] Evidence suggests that the core protein modulates some mitochondrial functions, including fatty acid β-oxidation, the impairment of which may induce lipid abnormalities and hepatic steatosis. In addition, the mitochondrion is an important source of reactive oxygen species (ROS). In livers of transgenic

Abbreviations: 2D-PAGE, two-dimensional polyacrylamide gel electrophoresis; COX, cytochrome c oxidase; ER, endoplasmic reticulum; Ero1, ER protein endoplasmic oxidoreduction-1; HCC, hepatocellular carcinoma; HCV, hepatitis C virus; HSP, heat shock protein; IFN, interferon; MnSOD, manganese superoxide dismutase; NS, nonstructural; OST48, oligosaccharyltransferases-48; PDH, pyruvate dehydrogenase; PDI, protein disulfide isomerase; ROS, reactive oxygen species; TFA, trifluoroacetic acid.

From the [1]Department of Internal Medicine, Graduate School of Medicine, University of Tokyo; [2]Department of Virology II, National Institute of Infectious Diseases, Tokyo, Japan.

Received June 17, 2008; accepted March 20, 2009.

Supported by a grant-in-aid for Scientific Research from the Japan Society for the Promotion of Science, from the Ministry of Health, Labour and Welfare of Japan (Research on Hepatitis), from the Ministry of Education, Culture, Sports, Science and Technology (Priority Area), from The Sankyo Foundation of Life Science, and from The Charitable Trust Araki Memorial Promotion Fund. T.T. is an awardee of the Research Resident Fellowship from the Viral Hepatitis Research Foundation of Japan.

Address reprint requests to: Kazuhiko Koike, M.D., Ph.D., Department of Gastroenterology, Internal Medicine, Graduate School of Medicine, University of Tokyo, 7-3-1 Hongo, Bunkyo-ku, Tokyo 113-8655, Japan. E-mail: kkoike-tky@umin.ac.jp; fax: (81) 3-5800-8799

Published online in Wiley InterScience (www.interscience.wiley.com).

DOI 10.1002/hep.22998

Potential conflict of interest: Nothing to report.

Additional Supporting Information may be found in the online version of this article.

mice harboring the core gene, increased ROS production has been observed.[7-9] A recent study found, by the proteomic profiling of biopsy specimens, that an impairment in key mitochondrial processes, including fatty acid oxidation and oxidative phosphorylation, and in the response to oxidative stress occurs in HCV-infected human liver with advanced fibrosis.[10] Therefore, it is probable that the HCV core protein affects mitochondrial functions because such pathogenesis is observed in both HCV core-transgenic mice and HCV-infected patients.[11-13]

The recent progress in proteomics has opened new avenues for disease-related biomarker discovery. Among proteomics approaches, two-dimensional polyacrylamide gel electrophoresis (2D-PAGE) is a technique for the separation and identification of proteins in a sample by displacement in two dimensions oriented at right angles to one another. This method is generally used as a component of proteomics and is the step used for the isolation of proteins for further characterization by mass spectrometry. 2D-PAGE is particularly useful when comparing two related samples such as healthy and diseased tissue. For example, proteins that are more abundant in diseased tissue may represent novel drug targets or diagnostic markers. In fact, several candidate biomarkers for many human cancers have been identified by this approach.[14] There are, however, tens of thousands of proteins in a cell, differing in abundance over six orders of magnitude. 2D-PAGE is not sensitive enough to detect rare proteins, and hence many proteins are not resolved. Therefore, splitting a sample into different fractions is often necessary to reduce the complexity of protein mixtures prior to 2D-PAGE. For this advantage, Lescuyer et al.[15] performed a 2D-PAGE of human mitochondrial proteins derived from the placenta and identified proteins mainly by peptide mass fingerprinting.

In this study, we performed a 2D-PAGE of mitochondria isolated from HepG2 cells stably expressing the HCV core protein and identified several proteins of different expressions when compared with control HepG2 cells. Among up-regulated proteins in the core-expressing cells, we focused on prohibitin, which functions as a mitochondrial protein chaperon, and found that the core protein interacts with prohibitin and represses the interaction between prohibitin and subunit proteins of cytochrome c oxidase (COX), which may lead to decreases in the expression level of the proteins and in COX activity. These results may explain the pathogenesis of liver disease in HCV infection including ROS induction.

Materials and Methods

Cells and Purification of Mitochondria. Hep39 cells,[16] which stably express the HCV core protein, and control HepG2 cells (Hepswx) were grown in Dulbecco's modified Eagle medium (DMEM) containing 10% fetal bovine serum and 1 mg/mL G418. Mitochondria were purified using Nycodenz (Nycomed Pharma, Zürich, Switzerland) according to the protocols reported by Okado-Matsumoto et al.[17] For transient transfection experiments, HepG2 cells were transfected with a core-expression plasmid using TransIT-LT1 (Mirus Bio, Madison, WI). Huh7 cells harboring HCV genotype 1b full-genomic (RCYM1)[18] or subgenomic replicon (5-15), and livers of 3-month-old core-gene transgenic mice[2] were also used for the analysis.

2D-PAGE. Gel electrophoresis in the first dimension was performed using an immobilized pH gradient gel (Immobiline Dry Strip gel, pH 4-7 linear, 13 cm; GE Healthcare, Uppsala, Sweden). The two-dimensional separation was performed on 12.5%, 14 × 16 cm^2, SDS polyacrylamide gels. After the electrophoresis, gels were silver-stained using a silver staining kit (GE Healthcare) according to the manufacturer's protocols. The stained gels were scanned and electronic images of the gels were analyzed using ImageMaster 2D Elite software (GE Healthcare).

In-Gel Digestion and Matrix-Assisted Laser Desorption Ionization, Time-of-Flight Mass Spectrometry (MALDI-TOF-MS). Protein spots on the gels were excised and a "control" piece was cut from a blank region of the gel and processed in parallel with the sample. In-gel digestion with trypsin was performed as reported.[19] The resulting peptides were concentrated using Zip-Tip C18 (Millipore, Bedford, MA). The peptide mixtures were eluted from Zip-Tip with 75% acetonitrile in 0.1% trifluoroacetic acid (TFA). The matrix (α-cyano-4-hydroxycinnamic acid dissolved in 50% acetonitrile, 0.1% TFA) was deposited on a dried sample target. Then 0.5-μL aliquots of the analyte solution were deposited onto matrix surfaces and the solvent was allowed to evaporate at ambient temperature. The digests were analyzed with a TOF mass spectrometer, PE Biosystems Voyager DE STR MALDI (Foster City, CA).

Database Analysis. For protein identification the measured monoisotopic masses of the peptides were analyzed using MS-Fit provided by UCSF (http://prospector.ucsf.edu/ucsfhtml3.2/msfit.htm).

Immunoblotting and Immunoprecipitation. Purified mitochondria were lysed and sonicated in RIPA buffer, then centrifuged at 16,000 rpm for 10 minutes. Protein concentration was determined using a BCA Protein Assay Reagent Kit (Pierce Biotechnology, Rockford, IL). The samples were separated by sodium dodecyl sulfate (SDS)-PAGE and electrotransferred onto a polyvinylidene fluoride membrane (Immobilon; Millipore, Japan), then blocked with BlockAce (Snow Brand, To-

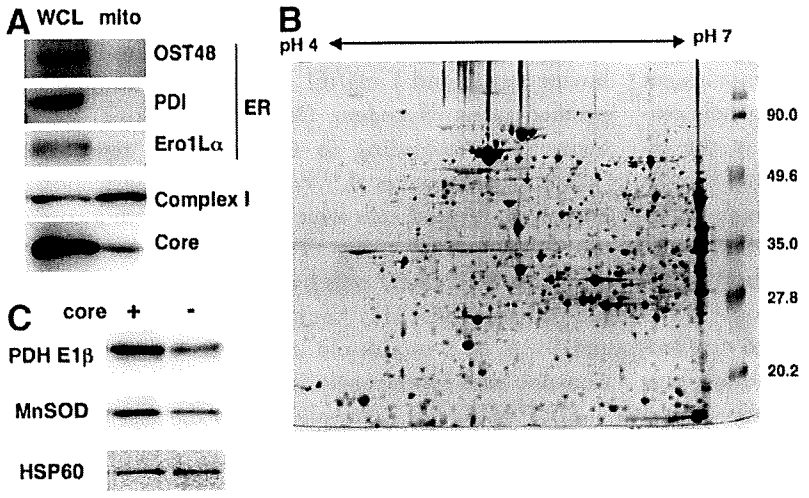

Fig. 1. 2D-PAGE of mitochondria purified from core-expressing cells. (A) Whole-cell lysates (WCL) and purified mitochondria (mito) derived from core-expressing cells were subjected to SDS-PAGE and immunoblotted with anti-core, anti-subunit of complex I (mitochondrial protein), or anti-OST48, PDI, Ero1La (ER proteins) antibodies. (B) Purified mitochondria of core-expressing cells were subjected to 2D-PAGE and the gel was stained with silver. The numbers shown on the right are molecular weights. (C) Purified mitochondria of core-expressing and control cells were subjected to SDS-PAGE and blotted with an anti-E1β subunit of PDH (PDH E1β), anti-MnSOD, or anti-HSP60 antibody.

kyo, Japan). The membrane was subsequently incubated with specific primary antibodies followed by horseradish peroxidase-conjugated secondary antibodies and visualized using SuperSignal West Pico Chemiluminescent Substrate (Pierce). Antibodies against the core protein (Anogen, Mississauga, Canada), manganese superoxide dismutase (MnSOD) (BD Biosciences, San Jose, CA), prohibitin (Neomarkers, Fremont, CA), oligosaccharyltransferase-48 (OST48), heat shock protein (HSP) 60 (Santa-Cruz Biotechnology, Santa Cruz, CA), pyruvate dehydrogenase (PDH), ubiquinol-cytochrome c oxidoreductase, COX (Molecular Probes, Eugene, OR), protein disulfide isomerase (PDI), ER protein endoplasmic oxidoreduction-1 (Ero1)-Lα, and IκBα (Cell Signaling Technology, Danvers, MA), were used as primary antibodies. For immunoprecipitation experiments, cells were lysed in NET-N buffer (20 mM Tris-HCl [pH 8.0], 100 mM NaCl, 1 mM EDTA, 0.5% Nonidet P-40) and the lysates were incubated with anti-prohibitin overnight followed by the addition of protein Sepharose 4B (GE Healthcare), then washed with the same buffer five times. Immunoprecipitates were subjected to SDS-PAGE followed by immunoblotting with specific antibodies.

Determination of COX Activity. COX activity was determined with a MitoProfile Rapid Microplate Assay Kit (MitoSciences, Eugene, OR) using 10 μg of purified mitochondria. The assay was performed three times independently.

Statistical Analysis. Results are expressed as means $\pm$ SE. The significance of the difference in means was determined by Student's t test or Mann-Whitney's U test.

Results

Presence of HCV Core Protein in Purified Mitochondria. Increasing evidence suggests that the HCV core protein is localized to mitochondria as well as to ER and the nucleus. Therefore, we first investigated whether the core protein is expressed in the mitochondria of core-expressing (Hep39) cells used in this study. We used Nycodenz discontinuous gradients to extract mitochondria as described.[17] In the mitochondria derived from core-expressing HepG2 cells, the core protein was detected by immunoblotting, whereas ER resident proteins such as an ER-specific type I transmembrane protein OST48, ER-resident molecular chaperon PDI, and ER membrane-associated N-glycoprotein Ero1-Lα, were not (Fig. 1A). In this fraction, reduced nicotinamide adenine dinucleotide (NADH)-ubiquinone oxidoreductase, complex I of mitochondrial oxidative phosphorylation system, was more strongly expressed than that in the whole cell. These results indicate that the purified mitochondria fraction was free of ER, and that a portion of the core protein was localized to the mitochondria in core-expressing cells.

Proteomics Analysis of Mitochondria by 2D-PAGE. For proteomics analysis, purified mitochondrial proteins derived from core-expressing cells were subjected to 2D-PAGE followed by silver-staining of the gel. In this study we analyzed only acidic proteins using IPG strips covering pH 4 to pH 7 because the analysis of acidic proteins by 2D-PAGE is relatively easy. The mitochondrial fraction was also extracted from Hepswx, a control cell line resistant to G418 but does not express the core protein, then similarly subjected to 2D-PAGE and used for comparing the expression pattern. We repeated the above procedure (purification of mitochondria, 2D-PAGE, and silver-staining) five times, and confirmed a similar expression pattern in core-expressing cells. The representative gel image is shown in Fig. 1B. ImageMaster 2D Elite software detected about 1100 spots on the silver-stained acidic gel, i.e., at pH 4-7 and Mrs of 20-100 kDa. The number of

Table 1. Proteins of Differential Expression in Mitochondria of Core-Expressing Cells

Protein Name	Fold Change (Mean ± SD)
Increased	
Succinyl-CoA:ketoacid CoA transferase	10.43 ± 1.29
NADH-specific isocitrate dehydrogenase a subunit precursor	9.64 ± 4.66
Unknown	8.65 ± 2.40
GrpE-like protein co-chaperon	5.71 ± 0.49
Leucine aminopeptidase	4.26 ± 1.14
Pyruvate dehydrogenase E1 component b subunit	3.79 ± 1.34
CGO15alt2	3.18 ± 0.80
HSP70	3.11 ± 1.39
Prohibitin	2.60 ± 0.24
3-Hydroxyisobutyrate dehydrogenase	2.47 ± 0.77
HSPC108	2.46 ± 0.69
MnSOD	2.35 ± 0.65
Ubiquinol-cytochrome c oxidoreductase core I protein	2.00 ± 0.23
Decreased	
Aldehyde dehydrogenase 2	0.12 ± 0.02
Aldehyde dehydrogenase 5 precursor	0.25 ± 0.03
ATP synthase a subunit isoform 1	0.50 ± 0.09
Reference protein	
HSP60	1.02 ± 0.02

protein spots was smaller than those reported in a recent study investigating the human placental mitochondrial proteome.[15]

We then compared the intensity of the spots between core-expressing and control cells. Analysis of repeated experiments by Student's t test revealed 13 increased and three decreased spots in intensity in core-expressing cells. These spots were excised and digested with trypsin, then proteins were identified by mass spectrometry. The names of the identified proteins are listed in Table 1. Among them were proteins related to mitochondrial respiratory chain, protein chaperons, and lipid metabolism. Because antibodies to some of these proteins are commercially available, expression levels of the proteins were examined by immunoblotting. The expression levels of the PDH-E1β subunit and MnSOD, which were identified as increased proteins, were higher in core-expressing cells than in control cells (Fig. 1C), whereas that of HSP60, which was identified as having a similar expression, was unchanged.

Up-regulation of Prohibitin by the Core Protein. Among the identified proteins, we focused on prohibitin, an up-regulated protein in mitochondria of core-expressing cells (Fig. 2A). Prohibitin is a mitochondrial protein associated with cell proliferation.[20] It also works as a chaperon of mitochondrial proteins.[21,22] We confirmed an increased prohibitin expression level in core-expressing cells

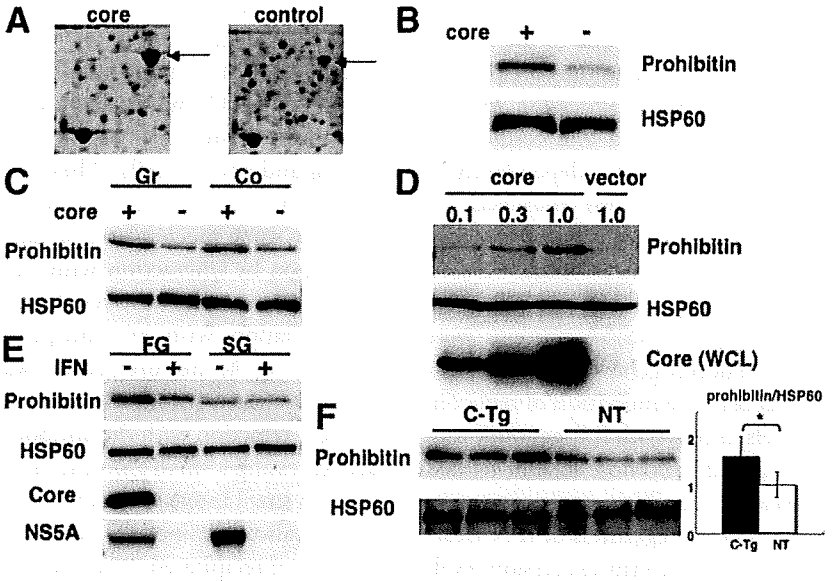

Fig. 2. Up-regulation of prohibitin in core-expressing cells. (A) Protein spot corresponding to prohibitin (arrow) in 2D-PAGE. (B) Purified mitochondria from core-expressing or control cells were subjected to SDS-PAGE and immunoblotted with anti-prohibitin or anti-HSP60 antibody. (C) Mitochondria were purified from growing (Gr) or confluent (Co) cells in 100-mm dishes and subjected to SDS-PAGE, then immunoblotted with an anti-prohibitin or anti-HSP60 antibody. (D) HepG2 cells in six-well plates were transfected with different amounts (μg) of core-expressing plasmid and mitochondrial proteins were analyzed by immunoblotting with anti-prohibitin or anti-HSP60 antibody. The expression levels of the core protein in whole-cell lysates (WCL) were also determined. (E) Cells harboring HCV replicon were untreated or treated with IFN and expression levels of prohibitin in mitochondria were determined. Expression of HCV core and NS5A proteins was also examined. FG, full-genomic replicon cells; SG, subgenomic replicon cells. (F) Expression levels of prohibitin in mitochondria were determined in liver tissues HCV core-gene transgenic and nontransgenic mice. Prohibitin/HSP60 expression levels were determined by densitometry. C-Tg, core-gene transgenic mouse; NT, nontransgenic littermate (n = 3) *$P < 0.05$.

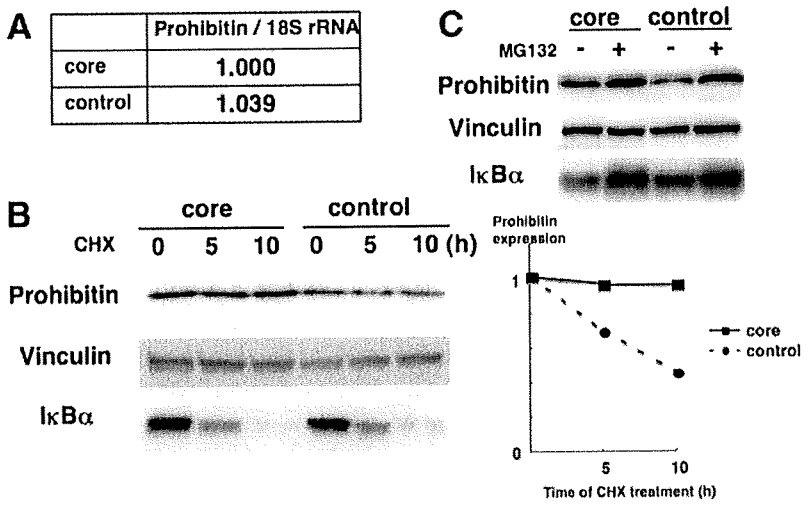

Fig. 3. Increased protein stability of prohibitin in core-expressing cells. (A) RNA was extracted from core-expressing and control cells, and the amount of specific mRNA was determined by real-time PCR with specific primers/probe against prohibitin. The amount of prohibitin mRNA was standardized by that of 18S ribosomal RNA (18S rRNA). (B) Cells were incubated with 100 ng/mL cycloheximide and harvested at the timepoints indicated above the lanes (numbers are hours of cycloheximide treatment). Whole-cell lysates were subjected to SDS-PAGE and immunoblotted with anti-prohibitin, anti-IκBα, or anti-vinculin (as an internal standard) antibody. The intensity of each band was measured by densitometry, and expression levels (prohibitin/vinculin) are shown in the right panel. (C) Cells were harvested after incubation with 20 μM MG132 for 8 hours and subjected to immunoblotting with anti-prohibitin, anti-IκBα, or anti-vinculin antibody.

by immunoblotting (Fig. 2B). Because prohibitin is associated with cell proliferation, it is possible that prohibitin expression changed according to the cell proliferative status. As shown in Fig. 2C, core-expressing cells had high prohibitin expression levels in the cells in both confluent growth and growing statuses compared with control cells. We also determined the expression levels in cells synchronized with aphidicolin followed by l-mimosine treatment and found an increased expression level in core-expressing cells (data not shown). To exclude the possibility that the increased prohibitin expression level is due to the expansion of limited cell clones, not specific to the core protein expression, we examined prohibitin expression in cells transiently expressing the core protein and found that prohibitin expression level increased dose-dependently in core-expressing cells (Fig. 2D). We also examined the prohibitin expression levels in Huh7 cells harboring full- or subgenomic HCV replicon. For this purpose, we used interferon (IFN)-treated replicon cells (cured cells) as a control. Core and nonstructural (NS)5A proteins were not detected after treatment of full-genomic replicon cells with IFN, suggesting a successful elimination of replicon. Prohibitin expression levels in cells with full-genomic replicon were increased compared with those in IFN-treated cured cells, whereas levels of prohibitin expression were low in subgenomic replicon cells regardless of IFN-treatment (Fig. 2E). In addition, prohibitin expression levels were also increased in livers of 3-month-old transgenic mice expressing the core protein compared with those in nontransgenic littermates (Fig. 2F).

We next sought to determine the mechanism of the increased steady-state level of prohibitin in core-expressing cells. To determine prohibitin messenger RNA (mRNA) expression, we performed a real-time polymerase chain reaction (PCR) using specific primers/probe. No difference in prohibitin mRNA was observed between core-expressing and control cells (Fig. 3A). We next determined the stability of prohibitin in these cells. By treating the cells with cycloheximide, the expression levels of prohibitin gradually decreased in control cells (Fig. 3B). On the other hand, in core-expressing cells prohibitin was hardly degraded by cycloheximide treatment for 10 hours, whereas IκBα was equally degraded in both cells. This result suggests that prohibitin was stabilized in the presence of the core protein. Because prohibitin has been shown to be degraded by proteasome,[23] we examined expression levels of prohibitin in the presence of proteasome inhibitor MG132. By treatment with MG132, prohibitin expression was increased to the similar level in core-expressing and control cells. These results suggest that the core protein may inhibit proteasomal degradation of prohibitin by some mechanism, including the prevention of degradation by interaction with the core protein. Then, core-expressing cells were lysed and subjected to immunoprecipitation with an anti-prohibitin antibody. As shown in Fig. 4, the core protein was coimmunoprecipitated with an anti-prohibitin antibody. To exclude a nonspecific interaction with the antibody or Sepharose beads, cells expressing a small amount of prohibitin by transfection with small interfering RNA (siRNA) against prohibitin were also examined. In these cells the amount of the coimmunoprecipitated core protein decreased. In addition, the core protein was not coimmunoprecipitated by control immunoglobulin G (IgG), indicating a specific interaction of prohibitin with the core protein. These results suggest that prohibitin expression increased in core-expressing cells owing to the increased stability presumably by interaction with the core protein.

Impaired Chaperon Function of Prohibitin in Core-Expressing Cells. We next examined the effect of

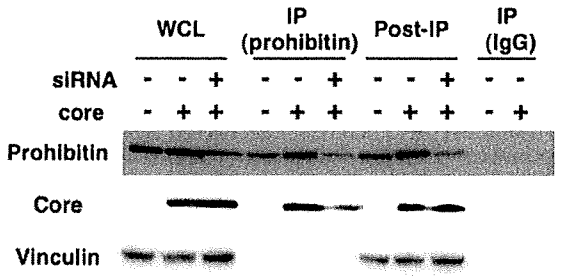

Fig. 4. Interaction of the core protein with prohibitin. Core-expressing and control cells were transfected with or without siRNA against the prohibitin gene, then harvested and lysed in NET-N buffer 3 days after transfection. Whole-cell lysates (WCL) were immunoprecipitated (IP) with an anti-prohibitin antibody or control IgG and immunoblotted with anti-prohibitin or anti-core antibody. Supernatants after the immunoprecipitation were harvested and similarly immunoblotted (Post-IP).

the interaction of prohibitin with the core protein on the function of prohibitin. Prohibitin works as a chaperon of mitochondrial proteins. Nijtmans et al.[21] demonstrated that prohibitin exerts a chaperon function particularly for the stabilization of mitochondrial DNA-encoded proteins. COX is a mitochondrial respiratory complex IV formed by 14 subunits, 10 of which are encoded by nuclear DNA and the rest by mitochondrial DNA.[24] We examined the interaction of prohibitin with subunit II of COX encoded by mitochondrial DNA. As shown in Fig. 5A, the level of COX II coimmunoprecipitated with an anti-prohibitin antibody was decreased in core-expressing cells, although the amount of immunoprecipitated prohibitin was higher than that in control cells. On the other hand, the subunit IV of COX encoded by nuclear DNA was similarly coimmunoprecipitated between core-expressing and control cells. When prohibitin expression was decreased by siRNA transfection, coimmunoprecipitation of COX subunits was similarly decreased with the amount of immunoprecipitation of prohibitin itself being low. We next determined expression levels of COX subunits in the mitochondria in these cells. Expression levels of mitochondrial DNA-encoded subunits I and II in core-expressing cells were decreased, whereas the levels of nuclear DNA-encoded subunits IV and VIb were similar to those in control cells. When transfected with prohibitin-siRNA, expression levels of all of the COX subunits examined were decreased in both core-expressing and control cells, suggesting that protein levels of these subunits are dependent on prohibitin (Fig. 5B, see Supporting Fig. 1 for densitometry). Similar data were observed when blots for COX II and IV were developed together in the same membrane (Supporting Fig. 2). We also determined COX activity in these cells and found that core-expressing cells had a significantly decreased COX activity (about 70% of that in control cells, Fig. 5C). These results suggest that interaction of prohibitin with the core protein is associated with an impaired function of prohibitin as a mitochondrial chaperon, which may trigger disordered assembly and function of mitochondrial respiratory complexes.

Discussion

In the present study we analyzed expression levels of mitochondrial proteins in HepG2 cells expressing the HCV core protein and identified a set of proteins with different expressions. Some of those proteins were related to the mitochondrial respiratory chain (Table 1). Because the core protein was shown to be associated with the induction of oxidative stress,[7-9] the core protein may modulate the expression and function of proteins forming mitochondrial respiratory complexes, which naturally

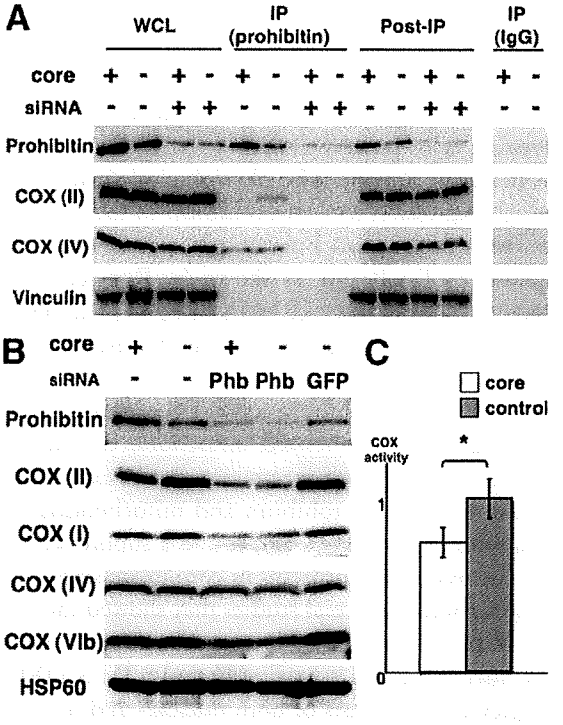

Fig. 5. Effects of core-prohibitin interaction on interaction/expression of COX subunit proteins and COX activity. (A) Whole-cell lysates (WCL) of core-expressing and control cells were subjected to immunoprecipitation with an anti-prohibitin antibody or control IgG, and the interaction of prohibitin with COX subunits was determined by immunoblotting of immunoprecipitated proteins (IP). Supernatants after the immunoprecipitation were harvested and similarly immunoblotted (Post-IP). (B) Cells were transfected with or without siRNA against the prohibitin (Phb) or GFP gene and harvested 3 days after transfection for purification of mitochondria. Purified mitochondria were subjected to SDS-PAGE and immunoblotted with several anti-COX subunits antibodies. The expression levels of HSP60 were also examined as an internal control. (C) COX activity was determined by measuring cytochrome c oxidation. The activity was normalized by taking the average rate of control cells as 1. Data shown are means ± SE ($n = 5$). *$P < 0.05$.